2023-05-01

Investigation Into The Roles Of Esxa N-α-Acetylation In Pathogenesis Of Mycobacterium Tuberculosis And Potential Host-Binding Proteins

Javier Aguilera
University of Texas at El Paso

INVESTIGATION INTO THE ROLES OF ESXA N-α-ACETYLATION IN PATHOGENESIS OF *MYCOBACTERIUM TUBERCULOSIS* AND POTENTIAL HOST-BINDING PROTEINS

JAVIER AGUILERA

Doctoral Program in Biosciences

APPROVED:

_____
Jianjun Sun, Ph.D., Chair

_____
Hugues Ouellet, Ph.D.

_____
Marc Cox, Ph.D.

_____
Lin Li, Ph.D.

_____
Siddartha Das, Ph.D.

_____
Stephen Crites, Ph.D.
Dean of the Graduate School

INVESTIGATION INTO THE ROLES OF ESXA N-α-ACETYLATION IN PATHOGENESIS OF *MYCOBACTERIUM TUBERCULOSIS* AND POTENTIAL HOST-BINDING PROTEINS

by

JAVIER AGUILERA, M.S.

DISSERTATION

Presented to the Faculty of the Graduate School of

The University of Texas at El Paso

In Partial Fulfillment

of the Requirements

for the Degree of

DOCTOR OF PHILOSOPHY

Department of Biological Sciences

THE UNIVERSITY OF TEXAS AT EL PASO

May 2023

Acknowledgements

This work would never have been possible without the support of my family, thank you for always being there for me and helping me develop professionally. I want to especially thank my mother, who has always worked tirelessly to provide for all her children and even those who are not in her immediate family. I have always admired her selflessness, work ethic and philanthropy and hope I can become as humble as she is.

I want to specially thank my mentor, Dr. Jianjun Sun for all his support throughout my academic career, when I first joined your laboratory, I had absolutely no experience but have learned many different techniques and have seen my greatest academic improvement through your teachings. My committee members, thank you all for helping me throughout my career and providing outstanding feedback toward the development of my project. Dr. Ouellet, thank you so much for always sharing your expertise and providing methods to improve our work. Dr. Li, thank you so much for your collaboration and everything you taught me in your computational biophysics course. Dr. Cox, thank you for always exemplifying great leadership and actively fostering collaborations. Dr. Das, thank you for being an excellent advocate and chiming in with your scientific curiosity, it was always insightful to hear your comments.

I also want to thank Dr. Elizabeth Walsh and Dr. Renato Aguilera, who were excellent advisors, as I could always count on your assistance. Although only my advisor for one semester, I also want to thank Dr. Spencer especially for your feedback for my presentation. I also want to thank my laboratory peers Dr. Salvador Vazquez Reyes and Dr. Pedro Jacquez, thank you for all your support throughout my career. Dr. Qi Zhang, thank you for serving as my first mentor who taught me all the basics of scientific research. Zeina Rhaim, thank you so much

for your support in my last semester at the university, I am sure you will achieve many great things. To all my undergraduate students particularly Elsa Rodriguez, Cynthia Lugo, Alexa Gallegos, and Maria Jose Rojero, thank you for all the hard work you did throughout your time in the laboratory. Finally, I would like to thank all my colleagues and friends for your support throughout my dissertation, it would not have been as pleasant of an experience. In particular, thank you to Alan, Angel, Briana, Diana, Isela, Olga, and Oscar.

This work was supported by the grant SC1GM095475 (J. Sun) from National Institute of General Medical Sciences, the grant 5G12RR008124 from the National Center for Research Resources and the grant 2G12MD007592 from National Institutes on Minority Health Disparities. This research was also supported by the grant R25GM069621 via the NIH RISE program for graduate students. This Research is also supported by University of Texas at El Paso new faculty start-up funds

Abstract

EsxA (6-kDa early secreted antigenic target, ESAT-6) is a critical virulence factor of *Mycobacterium tuberculosis* (Mtb). EsxA is secreted in a heterodimer with EsxB (10-kDa culture filtrate protein, CFP-10) through the Type VII secretion system of Mtb, called ESX-1. The dissociation of EsxA and EsxB heterodimer (EsxA:B), upon acidification, is required for EsxA to penetrate into the phagosomal membranes, which has been implicated in Mtb translocation from the phagosome to the cytosol. However, the mechanism of EsxA:B dissociation is not clear. In this study, we investigated the role of N-α-acetylation of EsxA in the heterodimer dissociation, mycobacterial cytosolic translocation, and overall virulence as well. Our results have demonstrated that N-α-acetylation of EsxA is required for the dissociation of the heterodimer at acidic conditions, which facilitates the mycobacterial cytosolic translocation. Subsequently, we also tried to identify the potential acetyltransferase of EsxA by gene bank search and tested if RimI, a potential N-α-acetyltransferase, acetylates EsxA *in vitro*. However, our data suggests that RimI does not acetylate EsxA. Inspired by a recent finding that EsxA may interact with the host mitochondrial receptors prohibitin 1 and 2 (PHB1 and PHB2), which plays a role in Mtb-regulated autophagy, we initiated a new study to express and purify the PHB1/2 proteins and characterize their interactions with EsxA. In summary, the study has revealed the mechanism of N-α-acetylation of EsxA in Mtb virulence and built the basis for future studies of EsxA interactions with host factors.

Table of Contents

List of Tables

List of Figures

Chapter 1: Introduction

1.1 Statistics of Tuberculosis Disease Caused by *Mycobacterium tuberculosis*

Mycobacterium tuberculosis (Mtb) is the causative agent responsible for the highly contagious infectious disease known as tuberculosis (TB). The World Health Organization (WHO) reported that in 2020, a staggering 10 million people across the globe were diagnosed with TB, and approximately 1.5 million fatalities were directly linked to this devastating disease (1). In fact, TB ranks among the top 10 causes of death worldwide and has the dubious distinction of being the leading cause of death resulting from a single infectious agent, even surpassing HIV/AIDS (1).

The symptoms of TB typically include persistent cough, high fever, significant weight loss, and recurring night sweats (2). Transmission of TB occurs through the air when an infected individual coughs, sneezes, or speaks, effectively releasing infectious droplets into the environment (3). These droplets are then inhaled by others who will be at risk of developing the disease. Importantly, TB is not spread through physical contact, such as shaking hands, sharing food or drinks, or kissing (3).

TB is more prevalent in low- and middle-income countries, where crowded living conditions and limited access to healthcare facilities contribute to its rapid dissemination. In 2020, 22 out of 30 nations with the highest TB burden were located in Africa (4). Alarmingly, an estimated 417,000 people in Africa succumbed to the disease in 2016 (4).

Individuals with compromised immune systems, such as those living with HIV, are at an elevated risk of developing TB (1,2; 5,6). This poses a further threat to Africa and other regions

where HIV/AIDS is prevalent (7). While TB is normally found as a pulmonary disease, it has the ability to infect beyond the lungs resulting in extra pulmonary tuberculosis (8).

1.2 Treatment of TB and the Rise of Antibiotic Resistance.

TB is generally treatable and curable by using a combination of antibiotics. However, the emergence of TB strains that display resistance to multiple antibiotics has compromised treatment efforts (9). The standard treatment regimen for TB involves a combination of several antibiotics administered for at least six months (10). First-line drugs for TB treatment, such as isoniazid and rifampin, are typically used in conjunction with other antibiotics, including ethambutol, pyrazinamide, and streptomycin (10). The latter three drugs are generally only prescribed during the initial two months of treatment.

Despite the existence of these treatment regimens, the rise of drug-resistant TB (DR-TB) poses a significant challenge to global health (1, 10). Treating DR-TB often requires more complex and longer interventions. Treatment of multidrug-resistant TB (MDR-TB) can last up to 20 months and necessitates the use of second-line drugs, which are not only more expensive but also associated with a higher incidence of adverse effects (11). Extensively drug-resistant TB (XDR-TB) is an even more severe form of TB that is resistant to multiple anti-TB drugs, including the two most potent first-line drugs, isoniazid, and rifampicin, as well as at least three second-line drugs used to treat drug-resistant TB (11,12).

Complicating matters further, cases of totally drug-resistant TB (TDR-TB) have been reported (13-15). This alarming development highlights the urgent need for novel therapeutic approaches to combat this increasingly drug-resistant and deadly disease. Continuous

dissemination of antibiotic resistant strains could have catastrophic effects (16). For this reason, the development of new treatment options is more critical now than ever before.

1.3 Current Vaccination Options

At present, the only vaccine available for TB is the Bacille Calmette-Guérin (BCG) vaccine, which was first developed in the early 20th century as a significant breakthrough in combating the disease. BCG is a live and attenuated vaccine administered as a single dose, typically at birth, and offers some degree of protection against severe forms of TB (17). Over time, BCG has become the only vaccine for TB prevention, owing to its reasonable efficacy and low risk profile (18, 19).

Nevertheless, there has been a longstanding interest in developing a more effective vaccine, as the BCG vaccine's effectiveness tends to wane over time (20-22). Moreover, revaccination with the BCG vaccine does not recover protection against TB (23-25). Encouragingly, several novel TB vaccine candidates are currently under development, with some even advancing to clinical trials (26).

One of the most promising candidates is the M72/AS01E vaccine, which demonstrated efficacy against TB in a Phase IIb clinical trial (27). Additional vaccine candidates in development include the VPM1002 vaccine, which is a recombinant BCG vaccine based on the EsxA and EsxB heterodimer (28). The continued exploration of these and other potential vaccine candidates as well as other preventive measures is crucial in the ongoing fight against TB and the development of more effective preventative measures.

1.4 Regions of Difference (RDs) Reveal Much About Mtb Virulence.

Comparative genomic analyses have uncovered several regions of difference (RDs) between the virulent Mtb strain H37RV and the attenuated strains, such as H37Ra and BCG (29-32). Thus, the RDs have become the focal points of TB research for the past decades, because a deeper understanding of the role of RDs in Mtb pathogenesis will pave the way for the development of innovative diagnostic, preventive and treatment strategies against TB (33).

Over time, the original samples used for the initial sequencing of Mtb were lost, necessitating the development of modern methods to establish a reference genome (34). These studies have identified a total of 10 regions of difference (RD1-10) within the Mtb genome. Among these regions, RD1 has emerged as the most heavily researched due to its association with virulence and the presence of the highly immunogenic antigens EsxA (ESAT-6) and EsxB (CFP-10) (35-39).

1.5 The Type VII Secretion System

Mtb has a variety of sophisticated and diverse secretion systems that are crucial for its pathogenesis and survival within host cells. Mtb utilizes these systems to deliver virulence factors, effectors, and other molecules to host cells, allowing it to manipulate host cell functions for its advantage. One of the most extensively studied secretion systems in Mtb is the type VII (T7SS), which consists of five unique ESX systems, each characterized by a specific set of components and substrate proteins (40-42). These ESX systems, labeled as ESX-1 through ESX-5, play vital roles in the virulence and survival of Mtb (43). Additionally, the ESX1-5 systems are composed of analogous structural proteins, with their primary distinctions being the effector proteins specific to each system (44).

The ESX-1 system is accountable for secreting the virulence factors EsxA and EsxB, which are crucial for lysing the phagosome membrane and enabling Mtb to escape into the cytosol of infected cells (45-47). As the most characterized ESX system in Mtb, ESX-1 is indispensable for Mtb pathogenesis. In contrast, ESX-2 and ESX-4 are the least studied, and their roles are largely unknown. While ESX-1, ESX-3, and ESX-5 are conserved, ESX-2 and ESX-4 are not as conserved across mycobacteria and are predicted to be non-functional (43, 48).

ESX-3 participates in the uptake of essential metals, such as iron and zinc, which are crucial for the growth and survival of Mtb within the host (49, 50). Investigations into ESX-3 have revealed that PPE4 is the most important PPE protein of Mtb for iron utilization (51). Finally, ESX-5 has been found to play a role in nutrient uptake by using PE and PPE proteins (52). ESX-5 has also been implicated in outer membrane permeability (53), seemingly due to the presence of the PPE25 and PE19 genes (54).

1.6 The ESX-1 Secretion System

ESX-1 is the most renowned among the ESX systems and is the central focus of this dissertation. As previously mentioned, ESX-1 is responsible for secreting several key virulence factors, including EsxA and EsxB (45-47). EsxA and EsxB are secreted as a heterodimer (EsxA:B), in which EsxA is a membrane-lytic protein, and EsxB is a molecular chaperone of EsxA (45, 46).

In addition to EsxA and EsxB, there are other essential virulence factors that are secreted by ESX-1, such as the Esp proteins, including EspA, EspC, EspD, EspE, EspF, EspG, amongst others. EspB protein is not found within the same operon, but it is still part of ESX-1 (43). Intriguingly, the expression of the Esp proteins is co-dependent on each other and on EsxA and EsxB (55-57).

In addition to all these proteins, ESX-1 also comprises several structural Ecc proteins, such as eccA, eccB, eccCa, EccCb, EccD, and EccE (43). These components work together to facilitate the function and secretion of virulence factors, which are crucial for the pathogenesis of Mtb.

1.7 EsxA:B Heterodimer Complex

EsxA and EsxB are the primary effectors of ESX-1 and play a significant role in manipulating the host immune response (35, 58). EsxA's membrane lytic activity is vital for the survival of Mtb within host cells. When a host macrophage phagocytizes Mtb, the bacterium can translocate from the phagosome to the cytosol due to EsxA's ability to form a membrane-spanning insert (47, 59).

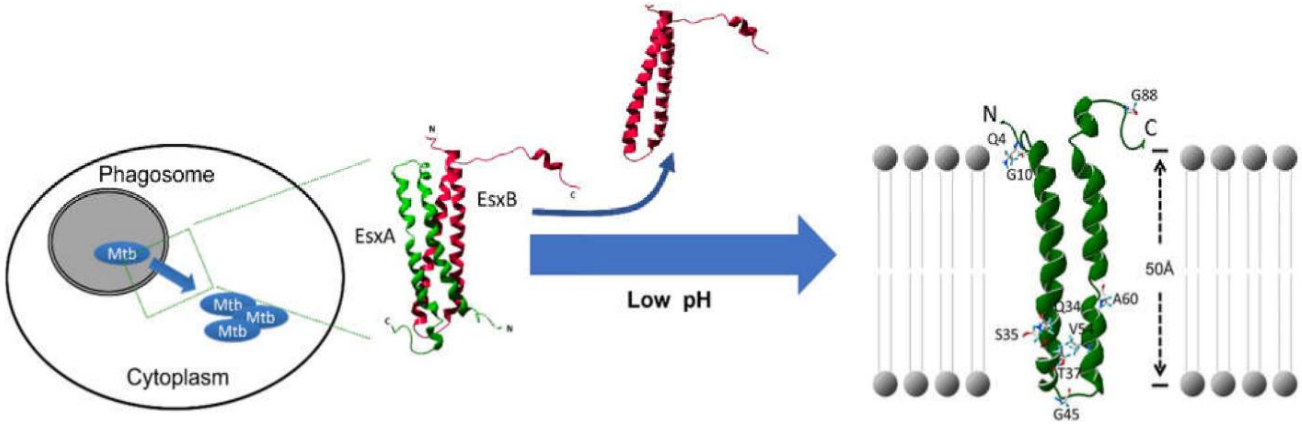

Figure 1. Proposed Model of Mtb Cytosolic Translocation Via EsxA (59, 60)

Following infection, Mtb encounters macrophages which phagocytize the bacteria. As it encounters acidic pH within the phagosome, EsxA dissociates from EsxB and forms a membrane spanning insert which allows Mtb to escape from the phagosome.

The exact mechanism of EsxA's cytolytic activity has been a topic of debate in various studies. Some research suggests that EsxA can only enact its cytolytic activity after dissociating from EsxB, which may be due to a change in pH within the phagosome, and subsequently gains the

ability to form a pore for cytosolic translocation (47, 61). On the other hand, other studies propose an alternative mechanism that may impact the membrane lytic activity of EsxA, suggesting that it does not depend on low pH (62, 63).

An earlier report, however, revealed the possibility of mycobacterial specific N-α-acetylation of EsxA could result in a change in EsxB's binding preference to EsxA (64). This finding leads to the hypothesis that the EsxA protein prepared from mycobacteria might have unique post-translational modifications that are not present in *E. coli*, potentially explaining the discrepancy in reported mechanisms of its membrane lytic activity.

1.8 N-α-Acetylation

N-α-acetylation is a post-translational modification that entails the addition of an acetyl group to the amino-terminal residue of a protein. This modification is catalyzed by a family of enzymes known as N-α-acetyltransferases (NATs) (65).

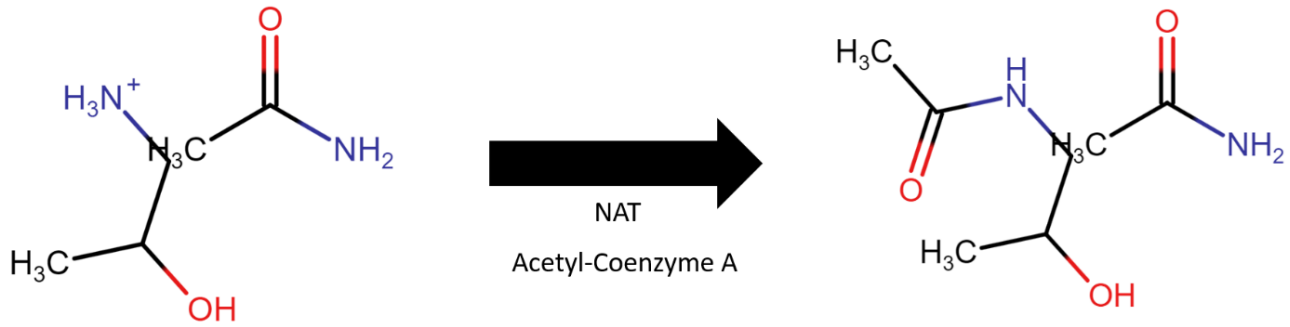

Figure 2. Diagram of N-α-Acetylation of Threonine Residue (66).

Acetylation occurs when an N-α-acetyltransferase transfers and acetyl group from acetyl-coenzyme A into the N-termini of a residue (threonine pictured), resulting in an acetylated residue and coenzyme A.

N-α-acetylation is among the most prevalent protein modifications in eukaryotes, with higher rates of acetylation observed in more complex organisms (67). This modification has been

linked to various cellular processes, including protein stability, protein-protein interactions, subcellular localization, and even acting as a molecular switch for protein activity (68-71). Recent studies have also identified the presence of N-α-acetylation in prokaryotes and its role in the pathogenicity of certain pathogens (72-74). However, N-α-acetylation has not been thoroughly studied in prokaryotes.

In our previous study, we have found that the EsxA:B heterodimer purified from *E. coli* does not exhibit membrane-lytic ability (45). The earlier report highlighting the absence of acetylation offers a compelling explanation for the discrepancies in the results obtained by different research groups (64). It is thus conceivable that N-α-acetylation may play a role in facilitating the heterodimer dissociation and enabling EsxA to engage in cell membrane lysis.

1.9 EsxA Interactions with Host Proteins

EsxA has been shown to interact with several host proteins, such as TLR2 (Toll-like receptor 2), which is a key receptor involved in recognizing bacterial pathogens (75). EsxA was also shown to interact with human syntenin-1, which is a scaffold protein involved in the regulation of various cellular processes, including cell migration, adhesion, signaling and involvement in the formation of exosomes (76). Recently, reports that EsxA interacts with host proteins have continued to increase (77-79).

Interestingly, EsxA was reported to have effects on the mitochondria of alveolar epithelial cells (80). Accordingly, EsxA can induce mitochondrial fragmentation as opposed to Mtb strains lacking EsxA. This evidence further supports previous studies that suggest EsxA plays a role in

autophagy (81). Altogether, EsxA appears to be a virulence factor with diverse roles and functions in pathogenesis.

1.10 Prohibitin-1 and -2 Proteins

One of the most important proteins within the mitochondria are prohibitins (PHBs), which are a highly conserved family of proteins found in eukaryotes. This family of proteins consists of two major proteins, prohibitin-1 (PHB1) and prohibitin-2 (PHB2). These two proteins share a considerable sequence similarity and form hetero-oligomeric complexes in various cellular compartments, particularly the inner mitochondrial membrane (82–84).

PHB1 was initially discovered as an anti-proliferative protein in mammalian cells and was predominantly localized in the mitochondria (84). PHB2 shares approximately 50% sequence similarity with PHB1 and is also primarily localized in the inner mitochondrial membrane. Together these proteins have been suggested to serve in the regulation of cell cycle progression, transcription, apoptosis, mitochondrial biogenesis, and cell signaling (85-89).

Why these proteins have so many roles is still not well understood. Part of their diversity is largely due to their ability to form oligomeric complexes, which can be as large as 20-25nm (75, 90). An earlier report indicated that prohibitins may act as a membrane bound chaperon for stability of mitochondria proteins (91). For this reason, PHBs may be involved in a variety of processes. Unfortunately, due to its versatility it may also be a key target for pathogens. It was discovered that prohibitin indeed served as a target for several pathogens, such as the Vi polysaccharide of Salmonella, nonstructural protein 2 of SARS-CoV, and as the target of Chikungunya virus receptor protein (92-94).

In conclusion, PHB1 and PHB2 are evolutionarily conserved proteins that play critical roles in maintaining cellular homeostasis, particularly in the context of mitochondrial function and cell cycle regulation. Their diverse roles have also been implicated in a number of infections. Given the essential role EsxA has in interactions with host mitochondrial membranes, it is reasonable to believe the prohibitins could interact with EsxA and serve as a pathway for the diverse role EsxA seems to play in tuberculosis infection.

1.11 Prohibitin-1 and -2 Interactions with EsxA

Previous studies have presented evidence indicating that EsxA may have direct interaction with host proteins, particularly those from the mitochondria (81, 82). Given that PHB1 and PHB2 play crucial roles in the cellular processes of the mitochondria, as well as serving as a target for multiple virulence factors in other pathogens (90-94), we decided to investigate further. Through a pulldown assay with the lysates of human lung epithelial cells (A549), we discovered that EsxA and EsxA:B pulls down with PHB1 and PHB2. Further exploration in our laboratory revealed that knockdown of PHB1 enhanced *Mycobacterium marinum's* invasion and upregulated its intracellular survival (95).

We believe that investigating this interaction is of significant value and lays the foundation to deciphering a key pathway in TB infection. Our findings strongly indicate PHB1 interacts with EsxA to regulate mycobacterial infection. Understanding the molecular mechanisms that govern their function and regulation will provide valuable insights into the development of novel therapeutic strategies targeting tuberculosis.

1.12 Significance

EsxA is a crucial virulence factor in *Mycobacterium tuberculosis*, possessing membrane lytic activity that contributes to Mtb's pathogenicity (47). The regulation of EsxA activity involves several factors, including N-α-acetylation, a post-translational modification with a previously studied role in pathogenesis (38, 56, 64). However, the precise impact of N-α-acetylation on EsxA interactions and its overall influence on virulence mechanisms in Mtb remains unclear. Investigating how N-α-acetylation affects EsxA's interactions with other proteins could provide crucial insights into the virulence mechanisms of Mtb.

A key aspect of this investigation is identifying the enzyme responsible for EsxA acetylation in Mtb. While previous studies have identified enzymes in *Mycobacterium marinum* that acetylate EsxA, the enzyme responsible for this modification in Mtb remains unknown (96). Determining the specific N-α-acetyltransferase that acetylates EsxA is critical to understanding this process in Mtb virulence. Identifying the enzyme could pave the way for the development of novel therapeutic strategies targeting Mtb.

Moreover, EsxA has been reported to interact with numerous host proteins, thereby eliciting a potent immune response (75-79). Notably, EsxA has been implicated in interactions with various host mitochondrial proteins (81,82). Our previous findings, which demonstrated EsxA pulled down with prohibitin-1 (PHB1) and prohibitin-2 (PHB2), highlight an intriguing interaction between these proteins (95). Given the multifaceted roles of the prohibitin proteins in host cells, exploring this interaction is of significant importance, as it may lead to the discovery of essential physiological pathways and broaden our understanding of Mtb pathogenesis.

1.13 Research Goal

EsxA holds several interacting partners which contribute to the pathogenesis of Mtb (75-79, 81, 82, 95). N-α-acetylation of EsxA, mediated by an as-yet unidentified N-α-acetyltransferase in Mtb, influences its interactions with binding partners, such as EsxB (64). These interactions are essential for the virulence mechanisms of *Mycobacterium tuberculosis* (96, 97). Investigating the effect of N-α-acetylation on EsxA interactions and identifying the specific enzyme which interacts with EsxA for this post-translational modification will provide valuable insights into the complex network of protein-protein interactions that contribute to Mtb pathogenesis. Furthermore, this may lead to the development of novel therapeutic strategies targeting these interactions. Moreover, the implications of EsxA interacting with host proteins reveal more about the pathways it exploits to aid MTB in pathogenesis. The discovery of possible interplay with prohibitin proteins further elucidates the diversity of EsxA. Therefore, the key goal of this study is to gain further insight into the complex network of EsxA interactions.

1.14: Specific Aims

1. Investigate role of N-α-acetylation of EsxA in virulence of Mycobacterium tuberculosis and its effect on the interaction with EsxB.
    a. Determine the state of acetylation of proteins previously generated containing Threonine 2 mutations.
    b. Confirm the effect N-α-acetylation has in the cell lytic activity of EsxA.
    c. Test whether the lack of a N-α-acetylation has an effect in Mtb virulence *in vivo.*
2. Identify and select possible enzyme(s) for catalyzing the N-α-acetylation of the EsxA protein via computational methods to express and purify them.

a. Research known N-α-acetyltransferases and use bioinformatics to cross reference them against proteins in Mtb.
b. Clone the gene from genomic DNA samples and insert it into an expression vector.
c. Express the gene and purify.
d. Carry out reaction and verify with DTNB qualitative method.

3. Express and purify prohibitin-1 protein to study its interaction with EsxA.
    a. Clone prohibitin-1 protein in expression vectors.
    b. Express and purify proteins on *E. coli.*

Chapter 2: Specific Aim I: 1. Investigate Role of N-α-acetylation of EsxA in Virulence of Mycobacterium tuberculosis and its Effect on the Interaction with EsxB.

2.1 Introduction

The success of Mtb as a pathogen is due, in part, to its ability to evade host immune defenses and establish long-term infections within host cells. The secretion of virulence factors is a key mechanism by which Mtb achieves these goals, and one such factor is the early secreted antigenic target 6 kDa (EsxA). Previous reports indicated EsxB had differential preference for binding between acetylated and un-acetylated EsxA (64). The purpose of this aim is to build on previous work done in our laboratory which confirms the state of acetylation in EsxA and its importance in virulence (96). We had previously generated EsxA with mutations at threonine2, the site of acetylation of EsxA, to study the effect of acetylation in the virulence of Mtb. In these mutants, the second threonine was mutated to an alanine (T2A), glutamine (T2Q), which were intended to serve as acetylation mimicking residues, and arginine (T2R), which was meant to function as an acetylation negative control (98, 99). It was later discovered these mutants did not behave in this fashion and therefore an additional serine mutant (T2S) was developed due to biochemical similarity to threonine and possibility of a different acetylation mechanism (100).

The importance of N-α-acetylation and its role in the pathogenesis of EsxA from Mtb was well established by our team. Additionally, others had also confirmed the effects of N-α-acetylation in *Mycobacterium marinum* (97). While the role of pathogenesis was clearly established, we

were unable to explain how N-α-acetylation affected the interaction of EsxA and EsxB. Initial attempts at comparing binding affinity showed some differences in binding affinity between acetylated and unacetylated EsxA but were inconclusive due to the difficulty binding the EsxB protein to a CM5 sensor chip (98). In this aim, we refined the effect N-α-acetylation had in the virulence of EsxA as well as to explain the difference acetylation had in the interaction of EsxA and EsxB.

In this study, we investigated the N-α-acetylation of EsxA in Mtb and its functional consequences. Through our team's development of *in vitro* separation of *Mycobacterium smegmatis* produced EsxA:B heterodimer, we were able to expand in the study of N-α-acetylation of EsxA and its effect in the interaction with EsxB (96). Using a combination of mass spectrometry, biochemical assays, and genetic approaches, we demonstrate that EsxA is N-α-acetylated. We further show that N-α-acetylation of EsxA is required for its stability, secretion, and cytotoxicity in macrophages. Our findings shed light on the post-translational regulation of EsxA and provide new insights into the mechanisms of Mtb pathogenesis. Understanding the role of N-α-acetylation of EsxA could lead to the development of novel therapeutic strategies for TB.

2.2 Methods

2.2.1 Generation of Proteins

2.2.1.1 Generation of EsxA Proteins from E. coli Expression Vector.

As previously described, EsxA proteins were generated in *E. coli* using the pET22b plasmid (75). Briefly, the T2A, T2Q, T2R, and T2S mutations were conferred into the EsxA gene via PCR and transformed into *E. coli* Bl-21 (DE3) cells and expressed (96). All proteins were then purified via

an on-column refolding protocol as previously described (98). For further purification a Superdex-75-containing column was used for size exclusion chromatography (SEC) and buffer exchange. Samples were concentrated using a 5,000MWCO vivaspin® until <5ml sample remained. The samples were then injected into the column and purified via an isocratic elution for > 1.5 column volumes (CV) with tris-buffered saline (TBS).

2.2.1.2 Generation of EsxA:B Heterodimer from M. smegmatis Expression Vector.

The EsxA:B heterodimer was expressed in *Mycobacterium smegmatis* using the pMyNT plasmid (98). The plasmids were transformed into the *Mycobacterium smegmatis* (Ms) Mc^2155 strain for expression (96). The proteins were then purified, as previously described, with few modifications (96). The proteins were sonicated at 70% amplitude using a ½ inch horn for a total of 10 minutes pulsing for 5 seconds and pausing for 10 seconds. After 5 minutes of sonication had elapsed, the sonication was paused, and cell lysate was allowed to cool down. The sonication was then continued until completion of the 10 minutes. Cell lysate was then centrifuged at 15,000 RPM for 45 minutes. The supernatant was passed through a pre-equilibrated Ni^{2+} column using a peristaltic pump. The samples were run through a gradient using an AKTA FPLC for a total length of 500ml and exchanging between 0%-70% buffer A (300mM NaCl, 10mM Imidazole 20mM Tris, pH 7.3) and buffer B (300mM NaCl, 500mM Imidazole, and 20mM Tris, pH 7.3). Following His-based purification the proteins were concentrated using a 5,000MWCO vivaspin® until <5ml sample remained. The sample was injected via injection loop into a Superdex-75 resin-containing column for SEC and buffer exchange through an isocratic elution > 1.5CV using TBS.

2.2.1.3 In vitro Separation of Ms Produced EsxA from EsxB Using 6M Guanidine.

EsxA:B heterodimer was concentrated using a 5,000MWCO vivaspin® until a concentration of nearly 5mg/ml was achieved. Guanidine was then added to the sample to a final 6M concentration. The sample was incubated overnight at 4°C. The proteins were then loaded into 2 Cytiva his-trap HP – 5ml columns connected in tandem. Elution was run through an AKTA FPLC in a 0-70% gradient with a total length of 150ml. The flowthrough was collected, containing EsxA, as well as the elution containing EsxB. Samples were exchanged into TBS via extensive dialysis.

2.2.2 Liposome Leakage Assay.

2.2.2.1 Liposome Preparation.

Liposomes for leakage assay were prepared as previously described (45, 101, 102). Briefly, 1,2-dioleoyl-sn-glycero-3-phosphocholine (DOPC) and 1,2-dioleoyl-sn-glyecro-3[(N-(5-amino-1-carboxypentyl)iminodiacetyic acid) succinyl] (Ni^+ salt) (DGS-NTA(Ni) were mixed at a 100:8 molar ratio and prepared as previously described (101). Alternatively, lipids were also produced at a 4:1 ratio of 1-palmitoyl-2-oleoyl-glycero-3-phosphocholine) (POPC) to 1-palmitoyl-2-oleoyl-sn-glycero-3-phospho-(1'-rac-glycerol) (sodium salt) (POPG).

2.2.2.2 ANTS/DPX Leakage Assay.

Prepared liposomes were rehydrated using 5mM HEPES, 50mM 8-aminonaphthalene-1,3,6 trisulfonic acid (ANTS) and 50mM *p*-xylene-bis-pyridinium bromide (DPX). The samples were subjected to 6 freeze-thaw cycles and extruded through a 0.2µm membrane filter a total of 20 times. The liposomes were desalted using a Cytiva HiTrap de-salting column into TBS. The desalted liposomes were mixed into a 1.5ml sample consisting of 100µl liposomes, 100µm NaAc, pH 4.0, and 150mM NaCl. The samples were loaded into an ISS K2 modulation

fluorometer with crossed polarizers on excitation and emission beams and a 435nm long path filter to reduce background scatter. After ~30 s, 100 µg of the protein was injected into the sample and fluorescence signal was monitored in real-time.

2.2.2.3 EsxA Titration Using EsxB.

ANTS/DPX liposomes were mixed into a 1.5ml sample consisting of 100µl liposomes, 100µm NaAc, pH 4.0, 150mM NaCl sample as well the pre-determined molar quantity of EsxB as compared to EsxA. The samples were loaded into an ISS K2 modulation fluorometer with cross polarizers on excitation and emissions as well as a 435nm long path filter. The reaction was initiated with 100 µg of EsxA being added after ~30s.

2.2.3 Detection of N-α-Acetylation Via NBD-Cl.

4-chloro-7-nitrobenzafurazan (NBD-Cl) was used for rapid detection of N-α-acetylation in the EsxA protein as previously described (96). Briefly, 6µl of the proteins were incubated with 0.5mM NBD-Cl in a 50mM sodium citrate and 1mM EDTA, pH 7.0 buffer. The reaction was monitored for 24 hours with measurements taken periodically with excitation at 460nm and emissions recorded at 535nm.

2.2.4 Mass Spectrometry

2.2.4.1 Sample Preparation.

FASP protein digestion (Expedeon, catalog no. 44250) was carried out using 100µg of each protein with trypsin (Sigma, catalog no. T6567) or pepsin (Sigma, catalog no. P7012). Briefly, the samples were resuspended in 200 µl of 12.48M urea, Tris-HCL solution (urea solution). Then, 10mg of dl-DTT was added to each sample and mixed in a nutating mixer for 45 minutes. Samples were then transferred to a 30-kDa filter and centrifuged at 14,000 RPM for 15 minutes.

Flow through was removed and 200 µl of urea solution was added to each spin filter and centrifuged at 14,000 RPM for 15 minutes. This step was repeated once more. Samples were then added 100µl of a 1:10 iodoacetamide to urea solution and incubated for 20 minutes without mixing in the dark. Afterwards, samples were spun at 14,000 RPM for 10 minutes. Flow through was discarded and the samples were washed twice with 100 µl urea solution. Urea was removed using 100 µl of a 50mM sodium bicarbonate solution 3 times, centrifuging at 14,000 RPM between each wash. Spin filters were transferred to a new collection tube and added 100 µl of either trypsin or pepsin at 0.02µg/µl. The samples were then incubated at 37°C for 18 hours. Peptides were eluted using 200µl of a 0.1% formic acid solution, and spun at 14,000RPM for 10 minutes. Digested peptides were frozen at -80°C for 2 hours and then lyophilized for 12 hours. The samples were resuspended into 100µl of 0.1% formic acid solution to a final concentration of 1µg/µl.

2.2.4.2 LC-MS/MS

Peptides, after trypsin or pepsin digestion, were analyzed by LC-MS/MS for 2 hours to 1 day using a QE Orbitrap and the Dionex UltiMate 3000 RSL Cnano UHPLC system in technical duplicates. A C18 PicoChip column (75-µm inner diameter X 15-µm tip packed with 10.5 cm of Reprosil PUR C18 3µm120 Å; 25µm X 50 cm fused-silica tail, New Objective) that was pre-equilibrated using solvent A (95% water, 5% acetonitrile, 0.1% formic acid) and solvent B (5% water, 95% acetonitrile, 0.1% formic acid) was used for loading of samples in line. The column was conditioned using 95% solvent A and 5% solvent B for 10 minutes with a 0.5µl/min flowrate. Peptides were eluted in a gradient to 40% solvent B for 95 min, followed by 10 min of 95% solvent B. The sample was re-equilibrated with 5% solvent B. Full-scan spectra were

collected using Xcalibur. Two blank injections were run in between samples using a 30-minute interval with seesaw washes using 5-80% solvent A to B gradients. QE Orbitrap settings were as follows: full MS resolution of 70,000, AGC target of 1e6, scan range from 400 to 1600m/z; MS/MS were run with a resolution of 17,500, AGC target of 2e6, scan range from 200 to 2000, and 3 m/z isolation window.

2.2.4.3 Bioinformatic Data Analysis

The resulting spectra were searched using Proteome Discoverer 2.1.1.21 and filtered via Sequest HT with an estimated false-discovery rate of 0.01 against sequences from *Ms* Mc^2155, *E coli* BL21, human, bovine, human keratin, and porcine trypsin. A 20-ppm precursor and 0.02 fragment tolerance were used. Cysteine carbamidomethylation, methionine oxidation, and lysine, threonine, serine, alanine acetylation was set fixed and variable modifications, respectively. The output files were manually analyzed and used to generate representative data.

2.2.5 Native Gel Shift Assay

Native gel shift assay was performed as previously described (45). Briefly, 1 µM of EsxB was incubated with varying concentrations of EsxA (0.5 µM, 1 µM, 1.5 µM, and 2 µM) at room temperature for a period of two hours. After the incubation period, the samples were subjected to native gel electrophoresis, using a 12% native gel. The separated proteins were then visualized using Coomassie Brilliant Blue staining.

2.2.6 Cytotoxicity Assay

Raw264.7 cells were cultured in Dulbecco's modified Eagle's medium (DMEM) containing 10% fetal bovine serum (FBS) with penicillin and streptomycin (100units/ml). Samples were kept at

37°C and 5% CO_2 until 60% confluent. Raw 264.7 macrophages were seeded in a 24-well plate with a density of 5.0 X 10^5/well for infection the following day. *Mycobacterium marinum (*Mm), an Mm strain containing knocked out gene MmΔEsxAB, and MmΔEsxAB strains complemented with EsxA:B and EsxA:B containing T2 mutations as previously reported (98), were cultured and prepared using a single cell preparation protocol (47, 103). Raw264.7 cells were then infected with Mm strains at a multiplicity of infection of 10 for 1 hour. During this hour cells were incubated at 30°C and 5% CO_2. The macrophages were then washed three times using phosphate buffered saline (PBS) to remove residual mycobacteria. The infected Raw264.7 cells were then incubated for another 3 hours at 30°C and 5% CO_2. The infected macrophages were then stained using calcein-AM and ethidium homodimer (Life Sciences) for 30 minutes. The samples were visualized under a fluorescent microscope for green cells (live) and red cells (dead). The number of dead cells were quantified from dozens of random fields from each sample. Images were processed using ImageJ.

2.2.7 CCF4-AM FRET Assay

Raw264.7 cells were plated in a 6-well plate at a density of 2.5 X 10^6/well in triplicate the day before infection. The cells were infected as previously described with few modifications (47, 104-107). Aspirate DMEM media and replace with EM media (7.02 g of NaCl, 0.52 g of KCl, 0.26 g of CaCl2, 0.076 g of MgCl, 0.9 g glucose and 6.5 of HEPES, pH 7.3 in 1L). Macrophages were infected at an MOI of 10 and incubated for 2 hours at 30°C and 5% CO_2. The infected raw 264.7 cells were washed 3 times to remove extracellular bacteria. Then, 2.5ml of pre-warmed EM media with 10% FBS was added, and cells were incubated for 48 hours. The macrophages were then probed with CCF4-AM according to the manufacturer's protocol (Liveblazer B/G loading

kit, Life Sciences). Samples were then excited at 409nm, and emissions measured at 450nm and 535nm. The *blue/green* ratio was calculated as I_{450}/I_{535}.

2.2.8 Molecular Dynamics Simulation

The 1WA8 structure for the EsxA:B heterodimer was downloaded from the Protein Data Bank (107). Protonation of states of ionizable residues at pH 4 and pH 7 were obtained using the DelPhiPka web server (108) and were assigned their respective states with visual molecular dynamics (VMD) (109). After removal of the first methionine, N-α-acetylation of was performed at the second threonine. The four structures, acetylated and unacetylated EsxA at either pH 4 or 7, were then solvated in water box with TIP3 (110) water model and ionized with 150mM NaCl in VMD. The final systems were simulated with the MD simulation program NAMD with each simulation performed for 20 ns employing a CHARMM27 force field (111, 112). Conditions were as follows: temperature 300K, pressure 1 atm. The snapshots from the simulations were taken to study the behaviors of the loop and flexible arm with and without acetylation at the second threonine.

2.3 Results

2.3.1 Acetylated EsxA:B Heterodimer Produced from *Mycobacterium smegmatis* (Ms) Contained Membrane Lytic Ability as Opposed to Non-Acetylated EsxA:B Heterodimer Produced from *Escherichia coli* (Ec).

We previously hypothesized the EsxA:B heterodimer produced from *Mycobacterium smegmatis* (Ms) would dissociate at low pH and be able to enact cell lysing ability as opposed to the heterodimer produced from *Escherichia coli* (Ec) (96). To test this, the two proteins were subjected to two different assays to evaluate the differences in their behavior in relation to their acetylation state.

Firstly, an ANTS/DPX dequenching assay was performed. In this assay, the ANTS and DPX dye pair is encapsulated inside a lipid membrane where, due to their close proximity, DPX quenches the fluorescence of ANTS. Upon lysis, ANTS is de-quenched and exhibits measurable fluorescence (Fig. 3A). The membrane-permeabilizing activity of the EsxA:B heterodimer produced from Ms was compared to the Ec-produced EsxA:B heterodimer using this assay. As predicted, the heterodimer produced from MS was able to permeabilize the liposome membrane at low pH, as opposed to the Ec-produced heterodimer (Fig. 3B).

Next, the proteins were assessed using a 4-Chloro-7-nitrobenzofuran (NBD-Cl) assay. NBD-Cl is a fluorophore that binds to the N-terminus of a protein at sites without N-α acetylation, resulting in fluorescence. In contrast, if a protein contains N- α acetylation, the fluorophore cannot bind, and no fluorescence is observed. Interestingly, the EsxA:B heterodimer purified from Ms did not exhibit fluorescence, suggesting the presence of N-α acetylation. This was in contrast to the heterodimer purified from Ec, which did exhibit measurable fluorescence (Fig. 3C). This result suggests that the Ms-produced heterodimer contains acetylation at the N-terminus as opposed to the Ec-produced proteins.

Collectively, these results indicate that the EsxA:B heterodimer from Ms and Ec exhibit different properties, with the Ms-derived protein appearing to have N-α acetylation, unlike its Ec-derived counterpart. This difference may contribute to the observed variation in their ability to lyse lipid membranes at low pH.

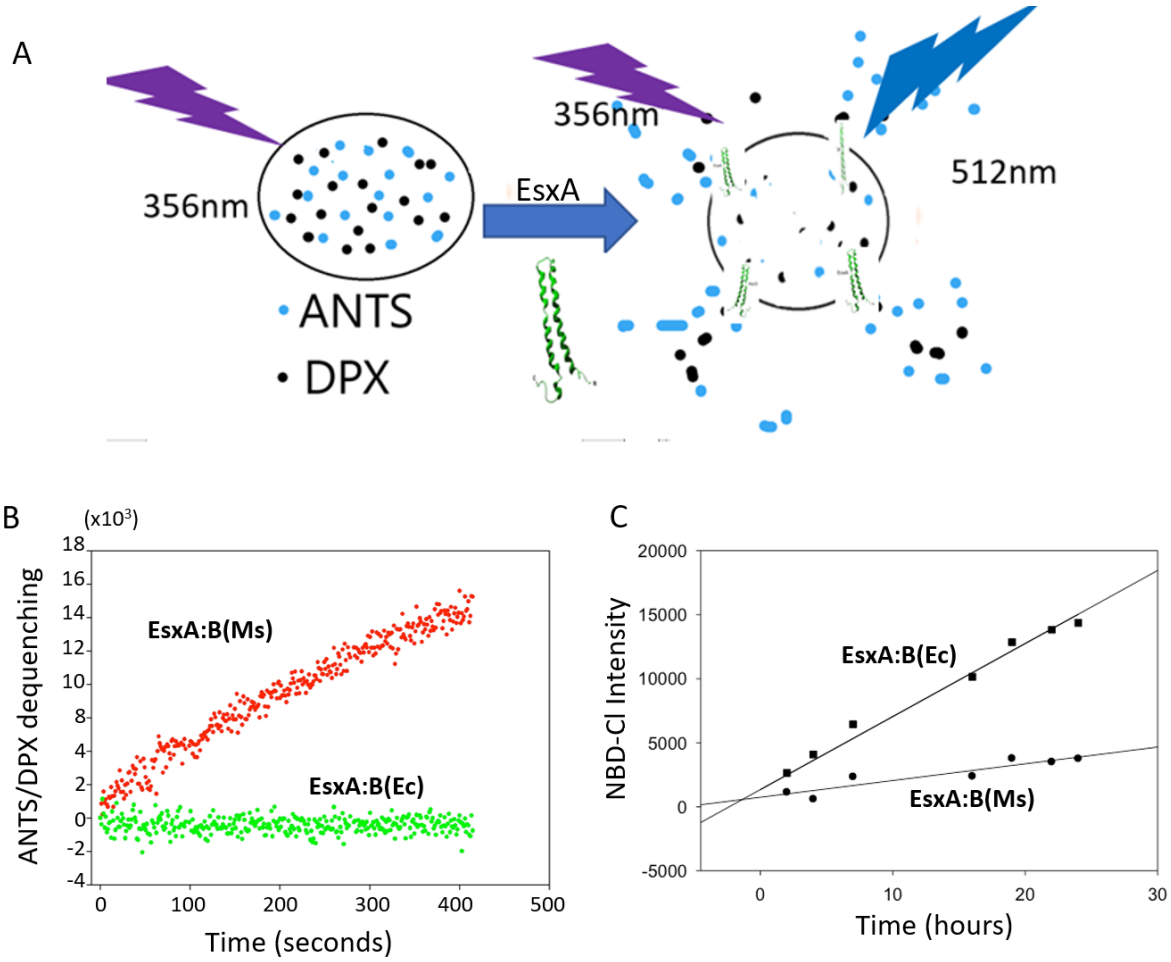

Figure 3. The EsxA:B Heterodimer Purified from Ms, but not in E. coli, Permeabilized the Liposomes at Low pH, Implicating the Role of N-α-Acetylation in Heterodimer Dissociation.

A) ANTS and DPX are encased within a liposome, and due to their close proximity, DPX suppresses ANTS fluorescence. When EsxA is introduced at a low pH, if the liposome membrane is lysed, ANTS will be separated from DPX, resulting in fluorescence. B) EsxA:B heterodimers purified from M. smegmatis (Ms) or E. coli (Ec) were evaluated in three separate experiments using the ANTS/DPX de-quenching assay at pH 4.0. C) Equivalent quantities of EsxA:B(Ms) or EsxA:B(Ec) heterodimers were exposed to NBD-Cl at room temperature. NBD-Cl is a fluorescent dye that specifically reacts with unacetylated sites, and its emission at 535 nm following 480 nm excitation can be plotted over time.

2.3.2 Mutations at Threonine-2 Abolished Cell Lysis Activity of the EsxA:B Heterodimer from Ms.

In previous studies, the alanine and glutamine residues were used to functionally mimic acetylation of a lysine residue, while arginine was used as a non-functional control. In our study we generated mutations at the second threonine (T2) of EsxA, by substituting the residue with either alanine (T2A), glutamine (T2Q) or arginine (T2R). These mutant heterodimer proteins from Ms were then tested using the ANTS/DPX dequenching assay. Unexpectedly, the results

revealed the heterodimers with the T2-mutations were not able to lyse the lipids containing the fluorescent pair as compared to the wild-type (WT) EsxA (Fig. 4A, B). This result suggested the mutations either blocked the separation of the EsxA:B heterodimer or blocked the membrane lytic ability of EsxA.

To confirm the mutations were not responsible for abolishing membrane lytic activity, we purified the EsxA proteins from *E. coli* containing the same mutations and revealed that the proteins were able to lyse the liposomes through the ANTS/DPX de-quenching assay (Fig. 4C,D). This result suggests the mutations did not abolish the membrane lytic ability of EsxA. Furthermore, this supports the hypothesis that the mutations blocked the heterodimer dissociation at low pH.

2.3.3 Separation of the EsxA:B Heterodimer

Prior to this study, there were no reports of the *in vitro* separation of the EsxA:B heterodimer. Successful separation was achieved using denaturing conditions with 6M guanidine as diagrammed (Fig. 5A). The previously co-purified heterodimer was subjected to denaturing conditions using 6M guanidine and was applied to a Ni^{+} affinity column for separation. The hexa-histidine tagged EsxB bound to the column and was eluted through an imidazole gradient, while EsxA was collected as flowthrough. The proteins were refolded using extensive dialysis and observed via SDS-PAGE (Fig. 5B).

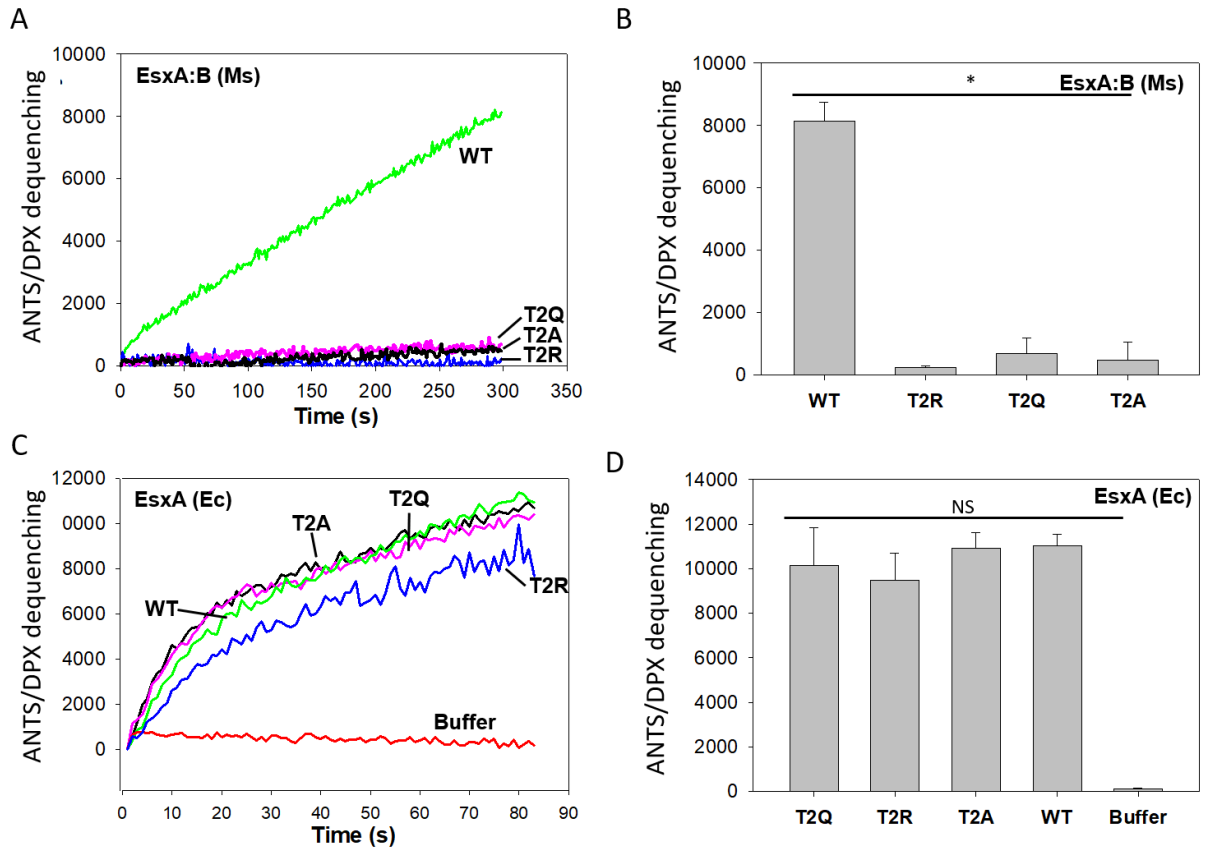

Figure 4. The Mutations at Thr-2 of EsxA Diminished the Membrane-Permeabilizing Activity of EsxA:B Heterodimer.

A) The EsxA:B heterodimer proteins (WT and mutants with T2A, T2Q, and T2R mutations) were purified from Ms. The membrane-permeabilizing capabilities of the purified heterodimer proteins were assessed using the ANTS/DPX fluorescence dequenching assay, with representative dequenching curves displayed. B) The mean endpoint fluorescence intensities from a minimum of three independent experiments were computed. The displayed results are the averages of three replicates, and error bars indicate standard deviation (S.D.). C) The EsxA proteins (WT and T2A, T2Q, and T2R mutants) were purified from Ec. The membrane-permeabilizing function of the Ec-EsxA proteins extracted from Ec was examined using the ANTS/PDX assay, and representative curves are provided. D) The average endpoint fluorescence intensities from at least three separate experiments were determined, with error bars representing S.D. NS denotes not significant.

2.3.4 N-α-Acetylation Is Absent in Mutants Lacking Membrane Lysing Ability.

As previous, the NBD-Cl assay was used once more to identify whether the T2 mutants contained acetylation. The Ms produced EsxA proteins were separated using 6M guanidine and compared to EsxA produced from Ec. Consistent with our previous result (Fig. 3C), the mutated EsxA proteins, which abrogated the activity of the EsxA:B heterodimer, did not contain N-α-

acetylation as determined by NBD-Cl. This was evident due to significantly higher fluorescence seen for all the mutants as opposed to the wild-type EsxA from Ms (Fig. 6A).

To validate the acetylation state of the mutants the Ms- produced EsxA wild-type (Ms-EsxA), Ms-EsxA (T2A), and Ec- produced EsxA wild-type (Ec-EsxA), were then subjected to LC-MS/MS. Additionally, due to its biochemical similarity a serine mutant was produced in Ms (MsEsxA(T2S)), and applied to LC-MS/MS. As expected, the Ms-EsxA contained acetylation, in addition to Ms-EsxA (T2S). Meanwhile the Ms-EsxA(T2A) and the Ec-EsxA did not contain acetylation (Fig. 6B). These proteins containing acetylation also had a methionine cleavage, distinctive to N-α-acetylation. Interestingly, other sites containing acetylation were discovered, although the roles of these modifications are not yet known.

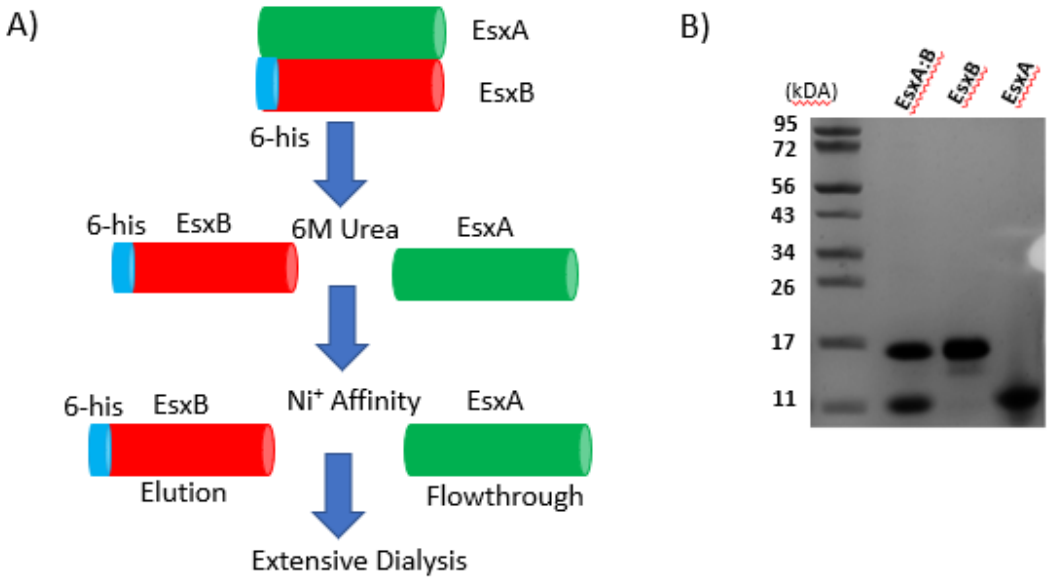

Figure 5. EsxA:B Heterodimer Was Separated *In vitro* Using 6M Guanidine.

A) Schematic depicting the procedure for separation of the EsxA:B heterodimer. The two proteins are bound via salt bridge, incubation with 6M guanidine disrupts that bond and allows for separation with nickel affinity. B) The EsxA:B heterodimer purified from Ms was separated by 6M guanidine, after which EsxA and EsxB were purified via nickel affinity.

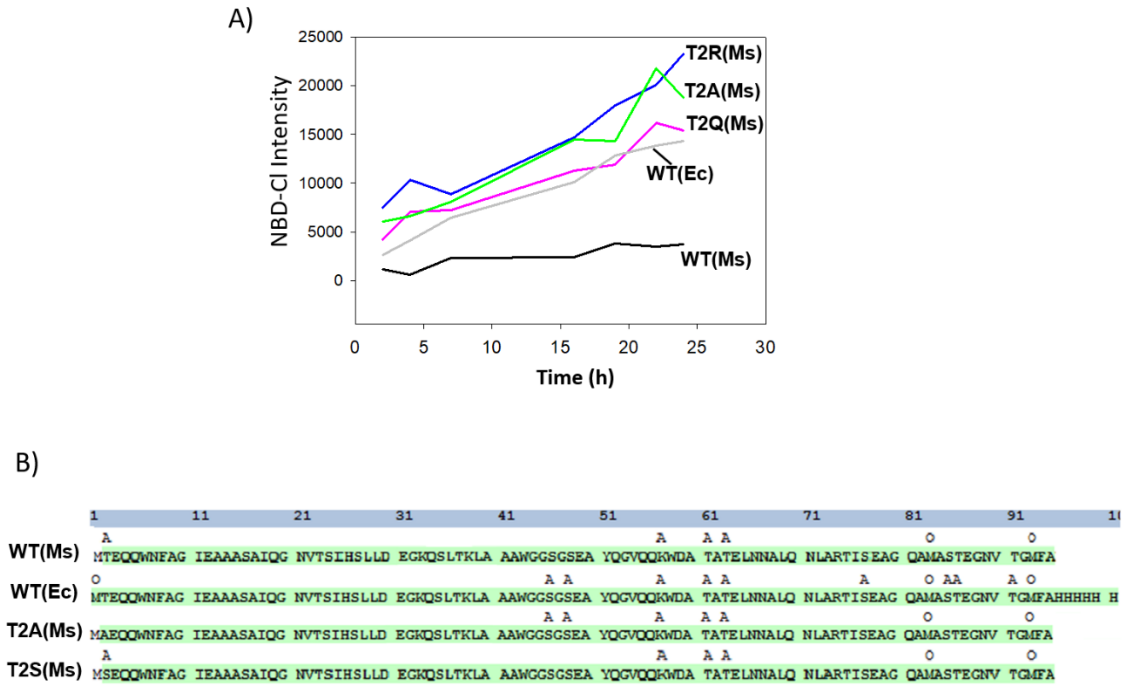

Figure 6. Detection of N-α-Acetylation of EsxA by NBD-Cl and LC-MS/MS.

A) The indicated EsxA proteins, purified from Ms, were incubated with NBD-Cl. At the indicated times, the fluorescence intensity of NBD-Cl was measured. B) The indicated EsxA proteins, purified from Ms or Ec, were analyzed via LC-MS/MS to identify the post-translational modifications. The residues with acetylation are labeled as A, and the residues with oxidation are labeled as O.

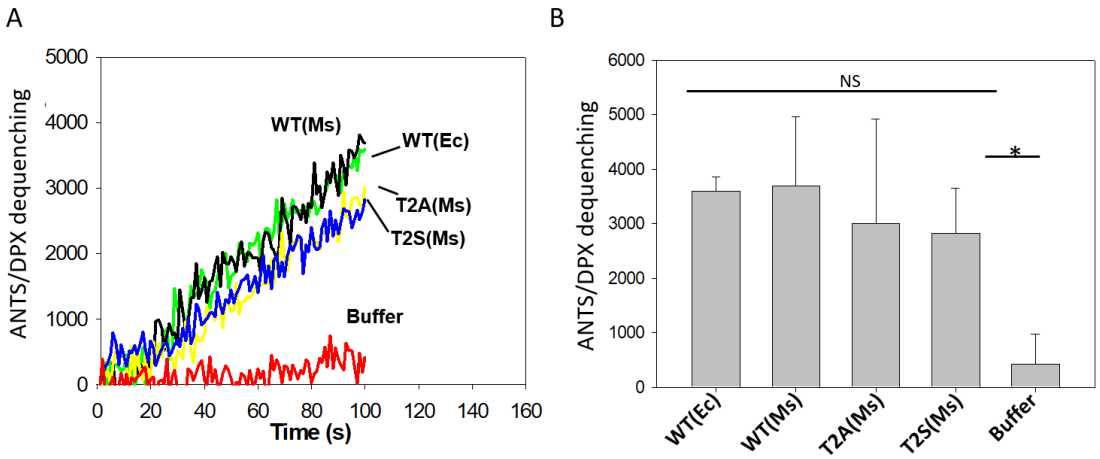

Figure 7. The N-α-Acetylation of EsxA Did Not Affect the Membrane-Permeabilizing Activity of EsxA.

A) The indicated Ms-EsxA proteins isolated from the Ms-heterodimer were tested for membrane-permeabilizing activity using ANTS/DPX assay. The Ec-EsxA (WT) protein, was used as a control. The representative curves from at least three independent experiments are shown. B) The average end-point fluorescence intensity from at least three independent experiments was calculated and is shown ($p < 0.05$).

2.3.5 Ms-Produced EsxA Regained Activity After Separation from EsxB.

Following the generation of *in vitro* separation of the EsxA:B heterodimer, the dissociated EsxA proteins were tested once more using the ANTS/DPX dequenching assay. The Ms-EsxA WT, Ms-EsxA (T2A), Ms-EsxA (T2S) were tested and the Ec-EsxA WT was used as a control for this assay. Through this experiment, it was revealed that upon *in vitro* separation, from EsxB, The EsxA protein was able to lyse cell membranes irrespective of the state of acetylation (Fig. 7A-B). Paired with the previous results (Fig. 4), this demonstrates the lack of N-α-acetylation is primarily linked to the inhibition EsxA:B heterodimer dissociation. Moreover, this result confirms the mutations do not inhibit the membrane-permeabilizing activity of the EsxA protein. Paired with the previous confirmation of acetylation states of the protein, this result validates that N-α-acetylation does not affect the activity of the EsxA protein.

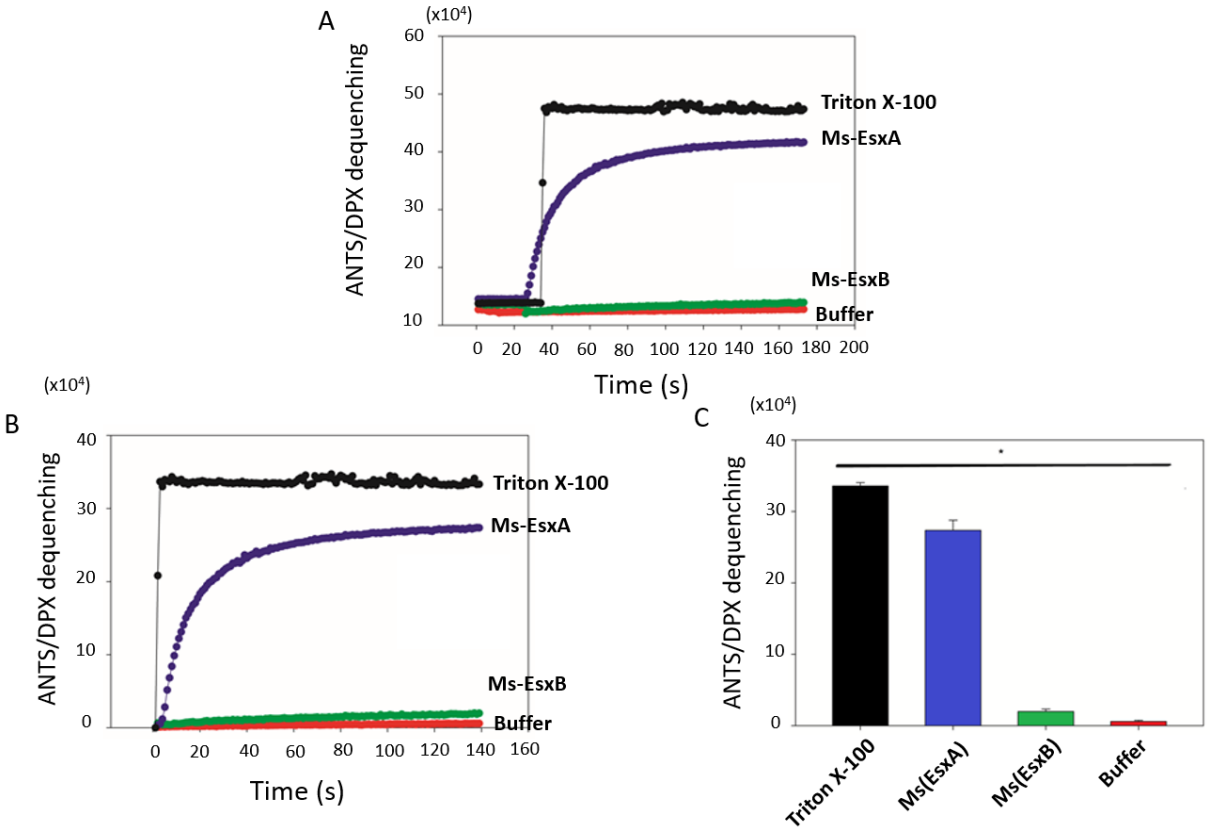

Figure 8. Generation of a Hyper-Sensitive ANTS/DPX Assay.

A) The Ms-EsxA and Ms-EsxB proteins isolated from the Ms-heterodimer were tested for membrane-permeabilizing activity using ANTS/DPX assay. Triton X-100 and TBS buffer were used as positive and negative controls, respectively. Representative curves from at least three independent experiments are shown. B) Data is transformed using the starting point of the assay to remove background light scatter. C) The average end-point fluorescence intensity from at least three separate experiments was calculated and is shown ($p > 0.05$).

2.3.6 Liposomes at a 4:1 POPC to POPG Resulted in an Optimized ANTS/DPX Assay for Measuring the Membrane Permeabilizing Ability of EsxA.

While ANTS/DPX assay has been extensively used by our group, we often noticed the sensitivity was not as high as opposed to other proteins (110). Therefore, we sought to optimize conditions to improve membrane permeabilizing ability of EsxA in liposome models. In a previous study we discovered membrane fluidity and charge contributed to the regulation of EsxA membrane insertion (113). Via a formulation of liposomes at a 4:1 ratio of 1-palmitoyl-2-oleoyl-glycero-3-phosphocholine) (POPC) to 1-palmitoyl-2-oleoyl-sn-glycero-3-phospho-(1'-rac-

glycerol) (sodium salt) (POPG), respectively (114) we observed intensities at x10^5 units (Fig. 8A). This represents nearly a 100-fold increase in sensitivity as opposed to the previous formulation (Fig. 7A).

After removal of scattered light, and data transformation at the moment liposomes were added to the experiment, a clear curve can be obtained and may even be useful in determining kinetics of EsxA (Fig. 8B, C). The new formulation resulted in the ability of EsxA to rupture the liposome membranes with nearly the same efficiency as Triton X-100. Furthermore, EsxB was once more tested using the new liposome formulation and maintains no activity. This result will facilitate future experiments using the ANTS/DPX assay for the study of membrane permeabilizing ability of EsxA.

2.3.7 EsxB Preferentially Bound to Nonacetylated EsxA and Inhibited Membrane Lysing Ability.

Given the EsxA:B heterodimer does not have membrane lytic activity we sought to reverse the reaction and incubate EsxB with EsxA. Furthermore, since a previous study found EsxB preferentially bound to EsxA in a 2-D overlay assay (64), we hypothesized EsxB would complex with EsxA and preferentially inhibit the membrane lysing ability of EsxA containing acetylation rather than the non-acetylated mutant. First, we used a native gel shift assay to determine whether the recently prepared proteins formed a complex. As expected upon incubation of the two proteins at different molar ratios of EsxA to EsxB, the EsxA:B complex was formed and led to the depletion of either protein at relative molar ratios (Fig. 9A).

Next, we applied the newly optimized ANTS/DPX assay to the EsxA (WT) and EsxA (T2A) mutant by incubating with EsxB at different molar ratios. Upon incubation with 0.5:1 molar ratio of EsxB to EsxA (T2A), the membrane permeabilizing ability of EsxA(T2A) was rapidly diminished

(Fig. 9B). Higher concentrations of EsxB, led to more inhibition of permeabilizing ability. On the contrary, at a 0.5:1 molar ratio of EsxB to EsxA(WT), a smaller decrease in inhibition was observed (Fig. 9C). The data from these experiments was normalized by using the maximum fluorescence observed from EsxA without EsxB, against the samples containing EsxB at different molar ratios. It was discovered that EsxB preferentially inhibited the liposome lysing ability of EsxA(T2A), which contained acetylation, as opposed to the non-acetylated EsxA(WT) at the 0.5:1 and 1:1 molar ratios (Fig. 9D).

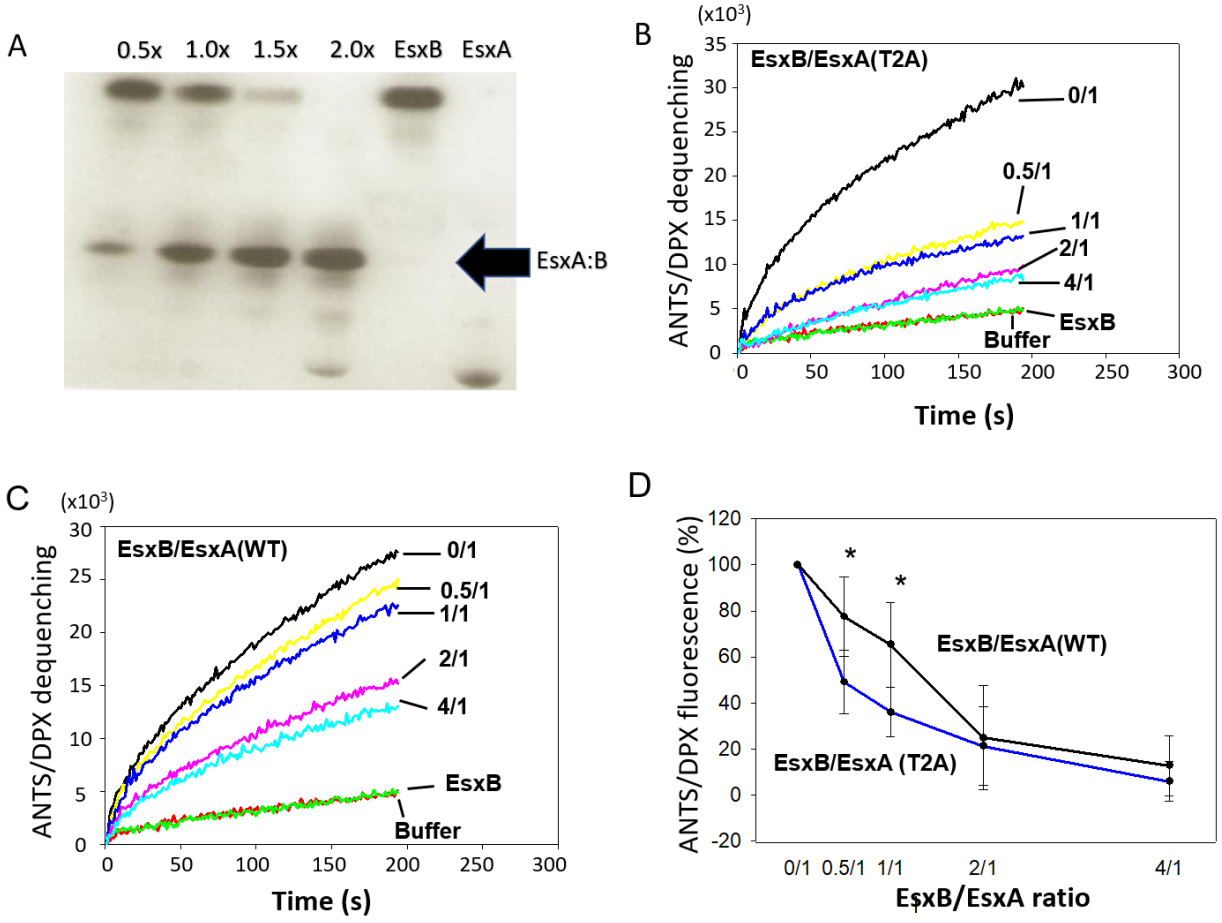

Figure 9. EsxB Preferentially Inhibited Nonacetylated EsxA(T2A) Over its N-α-Acetylated Counterpart.

The Ms-produced EsxA(WT) and EsxA(T2A) proteins were incubated with various concentrations of EsxB at the indicated molar ratios. The mixtures were tested in triplicate by the ANTS/DPX assay for membrane permeabilizing activity. The representative curves are shown in B and C, respectively. The relative inhibition from at least three independent experiments for a total n = 9 was summarized in D. For EsxA:B 0.5:1.0 ratio, $p < 0.0015$ and for EsxA:B 1:1 ratio $p < 0.0012$. Error bars represent S.D.

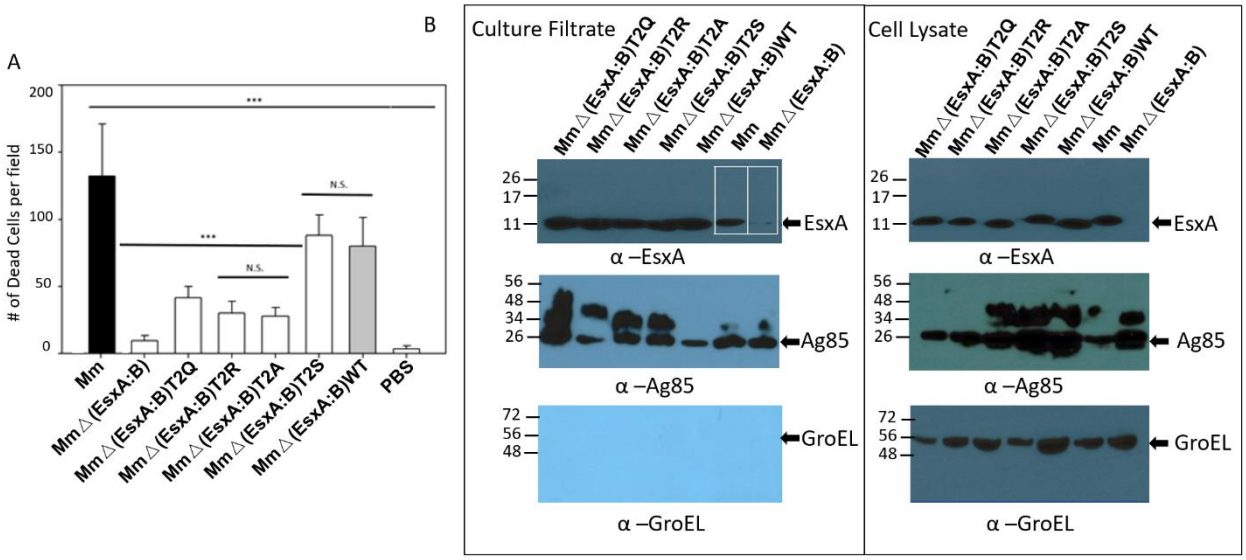

Figure 10. The Nonacetylated EsxA Diminished Virulence of *Mycobacterium marinum* Through a Cytotoxicity Assay.

A) RAW264.7 cells were infected with the indicated Mm strains at MOI of 10. The cytotoxicity was measured by using the live/dead assay. Dead cells were counted in random fields (***, n22,p <0.0001). B) EsxA proteins were found expressed in the total cell lysate and culture filtrate of the indicated *M. marinum* strains. GroEL was detected as a loading control for cell lysate and Ag85 was located as a loading control for culture filtrate.

2.3.8 The Mutations Without N-α Acetylation Attenuated Virulence of *Mycobacterium marinum.*

Next, we sought to investigate the effects of acetylation in pathogenesis of mycobacteria. The genes carrying the T2 mutations were inserted into the pMH406 vector. The genes were then expressed in a *Mycobacterium* marinum (Mm) strain in which the endogenous EsxB and EsxA operon was deleted (MmΔEsxA:B). Through a live/dead assay it was revealed the marinum strains carrying the T2-mutations lacking acetylation (MmΔEsxA:B(T2Q), MmΔEsxA:B(T2R), MmΔEsxA:B(T2A), had significantly lower cytotoxicity compared to the strains complemented with acetylation containing strains (MmΔEsxA:B(WT) and MmΔEsxA:B(T2S))(Fig. 10A). The wild type *Mycobacterium marinum* (Mm) was used as a positive control, the MMΔEsxA:B was used as a negative control, and a sample containing only phosphate buffered saline (PBS) was used as a vehicle control. The data confirms the lack of acetylation results in inhibition of mycobacterial pathogenesis and is consistent with a previous report (97).

To confirm the complemented strains were still capable of secreting the completement EsxA:B genes, the strains were subjected to immunoblotting. We found the mutations at T2 did not affect the expression, or secretion of EsxA:B heterodimer in the generated strains (Fig. 10B). Ag85 was probed using α-Ag85 antibody and was used as a loading control for culture filtrate and was observed in all strains. GroEL was probed using α-GroEL antibody and used as a loading control for cell lysate and was observed across all strains on cell lysate, but not expressed in the culture filtrate as expected.

2.3.9 Adaptation of CCF-4 FRET Assay for Investigation of Cytosolic Translocation of *M. marinum* in Raw264.7 Macrophages.

The previously developed β-lactamase reporter assay based on Förster resonance energy transfer (FRET) was applied in this study for investigation of the cytosolic translocation of Mycobacteria in macrophages (115, 116). More recently, this assay was applied to track *Mycobacterium tuberculosis* cytosolic translocation in THP-1 cells (104). We were particularly interested in applying it for use of *Mycobacterium marinum* (Mm) for the infection of Raw264.7 cells as the Mm strain is a safer BSL-2 pathogen (117). The assay utilizes CCF4-AM which contains 4-hydroxycoumarin and fluorescein bound via a lactam ring which when excited at 405nm sees a transfer of energy from 4-hydroxycoumarin to fluorescein emitting at 535nm (Fig. 11A). Upon infection with *M. marinum*, the macrophage will be endocytosed into a phagosome, and should the pathogen translocate, it will encounter CCF4-AM and cleave the lactam ring resulting in a loss of FRET, observable via emission at 450nm instead (Fig. 11A).

We applied this assay to wild-type *M. marinum* and *M. marinumΔEsxA:B* and discovered the wild-type strain was able to translocate from the phagosome into cytosolic space due the loss

of FRET and the emissions recorded at 450nm (blue light) (Fig. 11B). The *M. marinumΔEsxA:B* strain was not able to translocate from the phagosome as there was not shift in the peak emission spectra, and was consistent with a non-infected negative control. In order to quantify the difference, the emissions were recorded as a blue/green ratio as I_{450}/I_{535} (Fig. 11C, D). This assay will facilitate the investigation of cytosolic translocation of *M marinum.*

2.3.10 The Mutations Lacking N-α-Acetylation Reduced Cytosolic Translocation of *M. marinum* in Raw 264.7 Macrophages.

Using the adapted FRET assay, the Mm strains generated in this study were tested to see the effect the lack of N-α-acetylation has in the cytosolic translocation of *M marinum.* As expected, the results showed that the MmΔEsxA:B(T2Q), MmΔEsxA:B(T2R), and MmΔEsxA:B(T2A) strains reduced the ability of the mycobacteria's cytosolic translocation (Fig. 12). This was observed due to minimal loss of FRET as observed via low blue/green ratios. On the other hand, the acetylation containing MmΔEsxA:B(WT) and MmΔEsxA:B(T2S) complement strains were all capable of cytosolic translocation. Mm was used as a positive control, MmΔEsxA:B was used as negative control and PBS was used as a vehicle control. This experiment reveals the physiological effect of N-α-acetylation in Mm.

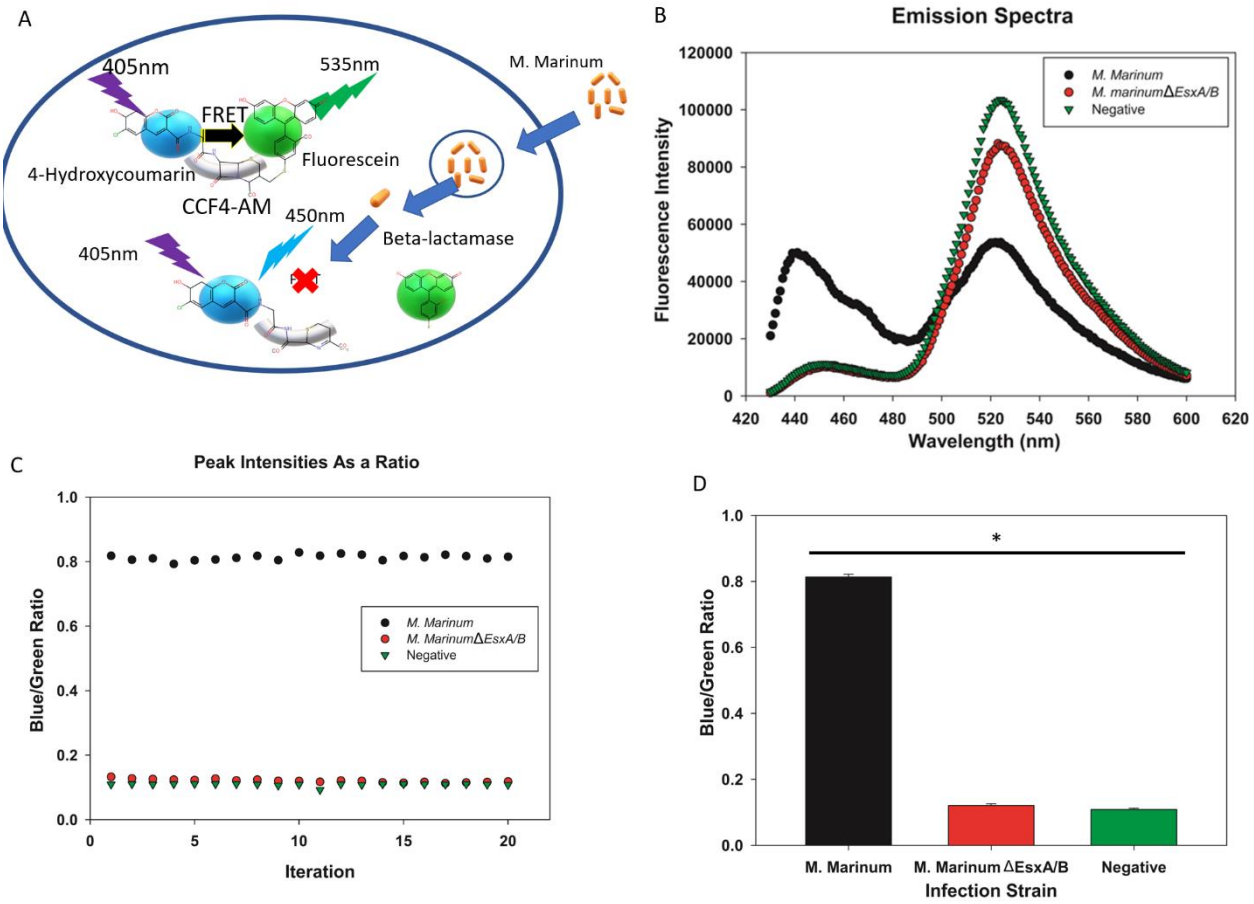

Figure 11. Adaptation of CCF4-AM FRET Assay for Study of Cytosolic Translocation of *M. marinum* in Macrophages.

A) The CCF4-AM FRET pair was internalized in macrophages. Upon infection with *M. marinum*, the bacteria are able to translocate into cytosolic space. The β-lactamase present on the mycobacterial cell wall is then able to cleave the lactam ring of the dye pair resulting in a loss of FRET. B) Emission spectra was recorded between 420 and 600 nm wavelengths. WT *M. marinum* had a higher number of emissions at ~450nm, showing cytosolic translocation. C) The blue/green ratio was measured by comparing emissions at 450 and 535 nm with excitation at 405 nm. D) The data were calculated from at least three independent experiments error bars represent SD (***, n = 3, $p < 0.0001$).

2.3.11 Molecular Dynamic Simulation Revealed a Bind and Release Contact Between Acetylated Threonine-2 and EsxB

Due to a lack of understanding of how N-α acetylation affects the structure of the heterodimer, we performed an MD simulation on the EsxA:B heterodimers with N-α acetylation and without acetylation in pH 7 and pH 4. As confirmed in this study, a low pH is required in order for EsxA and EsxA:B heterodimer mediated lipid lysis (Figs. 3-4, 6-7). Interestingly, at a neutral pH EsxB comes to close vicinity of EsxA without acetylation but is unable to make contact (Fig. 13 A, C).

The acetylated EsxA does not come into contact either and tends to be further away than EsxB at pH 7 (Fig. 13 B, D). At low pH the EsxB does not contact the un-acetylated EsxA (Fig.13 E, G). However, at pH 4, the acetylated EsxA is able to make direct contacts with EsxB in an interesting bind- and release- mode (Fig. 13 F, H). This finding reveals the importance of N-α acetylation in EsxA and EsxB interaction.

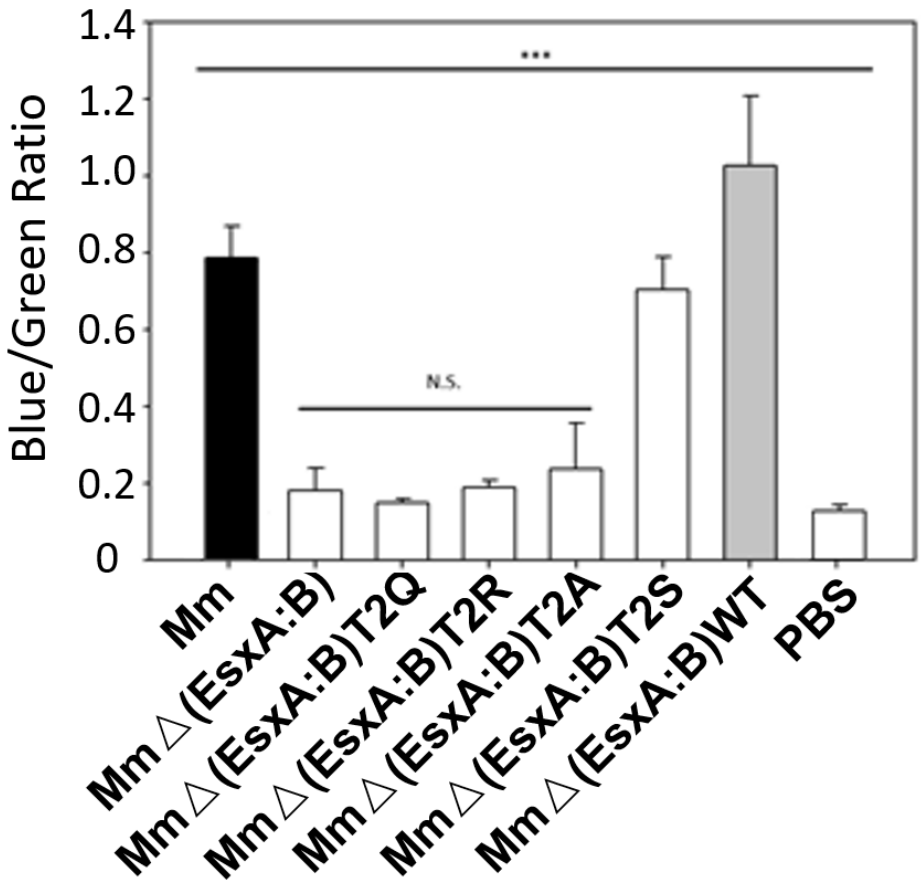

Figure 12. The Nonacetylated EsxA Reduced Cytosolic Translocation of *M. marinum*.

Mycobacterial cytosolic translocation was monitored by using CCF4-AM as a FRET reporter. The blue/green ratio was measured by comparing emissions at 450 and 530 nm with excitation at 409 nm. The data were calculated from at least three independent experiments error bars represent SD (***, n = 3, $p < 0.0001$).

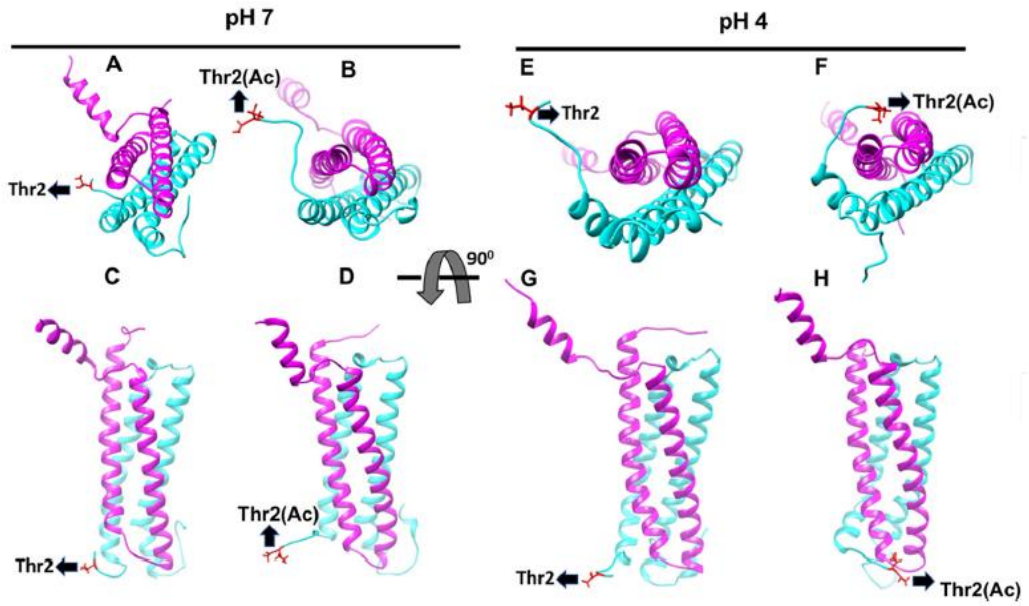

Figure 13. Molecular Dynamic Simulation Detects the Acetylated Thr-2(Ac) Interacts with EsxB in a Bind-and-Release Mode.

The structures of Mtb EsxA:B heterodimers with/out N-α-acetylation were analyzed by molecular dynamic simulation. The figures were generated from snapshots of 20-ns MD simulations at pH 7 and pH 4. EsxA, EsxB, and the Thr-2 residue are shown in cyan, pink, and red, respectively. The structures of EsxA:B heterodimer with non-acetylated Thr-2 at pH 7 and pH 4 are shown in A (pH 7, top view), C (pH 7, side view), E (pH 4, top view), and G (pH 4, side view), respectively. The structures of EsxA:B heterodimer with acetylated Thr-2(Ac) are shown in B (pH 7, top view), D (pH 7, side view), F (pH 4, top view), and H (pH 4, side view), respectively.

2.4 Discussion

In mycobacteria, EsxA and EsxB are co-expressed and co-secreted as a heterodimer. Previous studies have confirmed the essential roles of ESX-1, EsxA, and EsxB in mycobacterial cytosolic translocation and virulence (62, 104, 118, 119). Biochemical studies have demonstrated that EsxA has pH-dependent membrane-permeabilizing activity, whereas EsxB functions as a chaperone for EsxA (45). Current studies suggest the EsxA:B heterodimer is dissociated at low pH, which allows EsxA to permeabilize membranes (46). However, the mechanism of the heterodimer separation remains unclear. For the first time, this study found that N-α acetylation at Thr-2 of EsxA facilitates heterodimer separation at low pH, which allows EsxA to

permeabilize liposomal membranes and mediate mycobacterial phagosome escape and cytosolic translocation in macrophages.

The importance of EsxA and EsxB in mycobacterial pathogenesis is well-documented, with genetic manipulations that deleted the genes or abolished their secretion, attenuated virulence and inhibited phagosome rupture, cytosolic translocation, and cell-to-cell spreading (62, 104, 118-120). EsxA possesses a unique membrane-permeabilizing activity absent in its nonpathogenic ortholog *M. smegmatis*, and the secreted EsxA may penetrate the phagosome membranes during infection to facilitate mycobacterial cytosolic translocation (45, 46). In addition, mutations at the Gln-5 residue of EsxA have demonstrated up- or down-regulation of EsxA membrane-permeabilizing activity *in vitro*, affecting mycobacterial virulence and cytosolic translocation accordingly emphasizing the role of EsxA in membrane permeabilizing ability (47).

The study provides new evidence that the N-α-acetylation at Thr-2 of EsxA is required for mycobacterial virulence and cytosolic translocation by facilitating heterodimer separation. Although Thr-2 has no contact with EsxB in the reported solution structure of EsxA:B heterodimer, the MD simulation result generates an interesting model in which the acetylated Thr-2 has frequent bind-and-release contacts with EsxB at low pH, producing a dragging force to pull EsxB away from EsxA.

Protein N-α-acetylation is common in eukaryotes and plays crucial roles in protein-protein interaction, protein activity and stability, and cell growth and cell cycle (68-70, 121, 122). Over 100 proteins in Mtb have been found to be N-acetylated, including EsxA, and protein acetylation has been correlated with pathogenesis (123-125). However, little is known about N-

α-acetylation in bacteria, including mycobacteria. Further investigation is needed to understand the role of protein modifications in bacterial pathogenesis and to elucidate the mechanisms particular to *Mycobacterium tuberculosis.*

Chapter 3: Specific Aim II: Identify and Select Possible Enzyme(s) for Catalyzing the N-α-acetylation of the EsxA Protein via Computational Methods to Express and Purify Them.

3.1 Introduction

N-α-acetylation is a pivotal post-translational modification that plays a crucial role in the membrane lytic ability of the EsxA:B heterodimer and, consequently, has a significant impact on the virulence of *Mycobacterium tuberculosis* (Mtb). Notably, the second threonine residue of the EsxA protein is highly conserved across various strains (Fig. 14), emphasizing the importance of identifying the enzyme responsible for its acetylation. Uncovering the enzyme responsible for this modification could lead to the development of novel therapeutics targeting Mtb virulence, as suggested by previous studies (127).

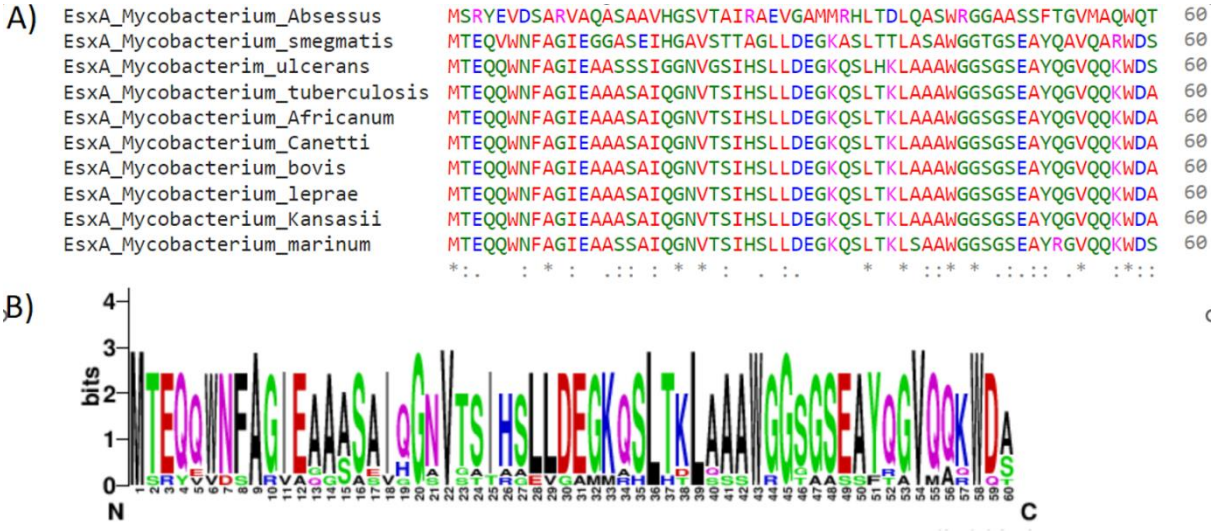

Figure 14. Multiple Sequence Alignment of the First 60 Amino Acids of Homologous EsxA Proteins.

A) Alignment of 10 EsxA proteins, performed with Clustal Omega (127), reveals a highly conserved threonine at the second position. B) Logo generated using weblogo from UC Berkley for clarity.

In other prokaryotes, several N-α-acetyltransferases (NATs) have been identified and characterized, including RimI, RimJ, and RimL in *Escherichia coli* (128). Interestingly, the genome of *Mycobacterium marinum* (Mm) contains a limited number of putative NATs, including the

identified MMAR_0039 protein which a study found to acetylate EsxA (97). However, in Mtb, no such orthologue exists raising the question as to what enzyme is responsible for the acetylation. Recently, another study revealed Mtb possess the RimI NAT and appears to produce relaxed substrate specificity (129).

In this aim, our primary objective is to identify the NAT responsible for the modification of EsxA. We will use bioinformatics to identify candidate enzymes in Mtb that may be involved in the N-α acetylation of EsxA. In parallel we will use biochemical approaches to express and purify the candidate enzyme capable of modifying EsxA. Additionally, we will perform *in vitro* acetylation assays to screen for candidate enzymes that can modify EsxA. In conclusion, this study will provide important insights into the regulation of EsxA and the pathogenesis of tuberculosis.

3.2 Methods

3.2.1 Bioinformatic Study of Possible NAT Proteins

RimI, RimJ, RimL sequences from *Pseudomonas aureginosa* were downloaded from NCBI protein bank. A BLAST(p) analysis was run against *Mycobacterium tuberculosis* (taxid: 1773). Representative data of each blast was stored. The MMAR_0039 protein was input into the conserved domain search. The conserved domain was then used to compare to the RimI, RimJ, and RimL sequences using Clustal-OMEGA. The generated file was then analyzed using MView.

3.2.2 Construction of Vectors

RimI gene was isolated from genomic Mtb DNA via PCR. PCR samples were purified using a PCR clean up kit (Thermo Cat#K310001). The RimI gene was cloned into the NdeI and XhoI sites into pET22b, pET28b, and pCold-TF vectors. Additionally, the RimI gene was inserted into the BamH1 and EcoRI site in pGEX-4T-1. All constructs were verified using DNA sequencing.

Table 1. Primers Used for Generation of Vectors Containing the RimI Protein.

List of primers used in the study for cloning the RimI protein into the pET22b, pET28b, pGEX4t-1 and pCOLD-TF vectors.

Vector	F-Primer	R-Primer
pET22b	ATGCCATAGCCTGACGGCCGACACCGAGCC	ATGCCTCGAGTTATGACGGGTCCCCCGAATCCC
pET28b	ATGCCATAGCCTGACGGCCGACACCGAGCC	CCGCTCGAGTCATGACGGGTCCCCCGAATCCC
pGEX-4T-1	ATGCGGATCCATGGTGACGGCCGACACCGAGCC	ATGCCTCGAGTCATGACGGGTCCCCCGAATCCC
pCOLD-TF	CATATGGTGACGGCCGACACCGAGCC	AAGCTTTCATGACGGGTCCCCCGAATCCC

3.2.3 Optimization of Purification Conditions.

3.2.3.1 Expression in pET22b, pET28B, or pGEX-4t1 Plasmid.

The expression of RimI protein was analyzed using the pET22b, pET28b, or pGEX-4t-1 plasmid in *E. coli* BL21(DE3) strain. A single colony of transformed bacteria was inoculated into 5 mL of LB broth supplemented with carbenicillin. The cultures were incubated overnight at 37°C with shaking at 220 RPM. The overnight culture was then used to inoculate 50 mL of LB broth supplemented with carbenicillin at a final concentration of 100µg/ml in a 250 mL flask. The sample was grown at 37°C with shaking at 220 RPM until the OD_{600} reached 0.6 to 0.8. The expression of RimI protein was induced by addition of IPTG to the culture at a final concentration of 1 mM and continuing to shake at varying temperatures, RPM, and time as described in the tables below (Table 2 and 3). The bacteria were harvested by centrifugation at 5,000 x g for 10 minutes at 4°C. The cells were lysed using 300µl of bacterial protein extraction reagent (B-PER^{tm}). A 50 µl sample was retained to observe the total lysate sample, the remainder was centrifuged at 15,000RPM for 10 minutes at 4°C to collect the insoluble fraction,

found in the pellet, as well as the soluble fraction, supernatant. All samples were loaded into an SDS-PAGE for analysis.

3.2.3.2 Expression of RimI in pCold-TF Plasmid.

The expression of RimI protein was analyzed using the pCold-TF plasmid in *E. coli* Lemo21 strain. The samples were grown usings similar conditions to the previous plasmids but also contained varying concentrations of L-rhamnose.

3.2.4 Purification of RimI Protein.

The RimI containing pCold-TF vector was expressed into *E. coli* Lemo21 cells. For protein expression, a single colony was inoculated into 5 ml LB broth containing 100 µg/ml carbenicillin and incubated overnight at 37°C with shaking at 200 RPM. L-rhamnose was added at a final concentration of 500µg/ml to tune for soluble expression. The overnight culture was then used to inoculate 1L of LB broth containing 100 µg/ml carbenicillin and grown at 37°C with shaking at 200 RPM until the OD_{600} reached 0.6. The cells were induced with IPTG to a final 1mM concentration and incubated at 16°C while shaking at 200 RPM for 48 hours. The cells were harvested by centrifugation at 8000 RPM for 10 minutes at 4°C. The cells were resuspended in buffer A (300Mm NaCl, 10mM imidazole, 20mM tris, pH 7.3) containing a protein inhibitor cocktail (Pierce™ Cat #32965) and sonicated on ice for 10 minutes pulsing on and off for 5 seconds and 9 seconds, respectively. The cell lysate was then centrifuged at 15,000 RPM for 45 minutes at 4°C to remove cell debris. The clarified cell lysate was loaded onto two 5mL HiTrap™ TALON® crude columns (Cytiva Cat# 28953766) connected in tandem using a peristaltic pump. The protein was eluted using an AKTA FPLC, pre-equilibrated with Buffer A and Buffer B (300mM NaCl, 10mM imidazole, 20mM tris, pH7.3), on a 100mL gradient from 0% - 70% Buffer

B. The eluted protein fractions were concentrated using a 30,000MWCO Vivaspin®. The concentrated protein sample was injected into an AKTA FPLC into a superdex-200 column for size exclusion chromatography and buffer exchange.

3.2.5 DTNB Quantitative Assay.

A DTNB assay was performed as before with few modifications (129). In a 100µl sample acetylation reactions were carried out using 0.5mM acetyl CoA, 4mM peptide substrate or protein, in a 50mM tris buffer pH 8.0. The reaction was initiated by the addition of 8µM or 4µM RimI. The samples were incubated at 25 °C for one hour. The reaction was ended by addition of 60µl of a 3.2M Gn-Hcl solution. Then, 10µl of a 2mM DTNB solution was added, mixed, and incubated for 5 minutes. The absorbance at 412nm was measured and total product was calculated using a CoASH standard curve.

3.3 Results

A

- Rim I:

Description	Scientific Name	Max Score	Total Score	Query Cover	E value	Per. Ident	Acc. Len	Accession
ribosomal protein S18-alanine N-acetyltransferase [Mycobacterium tuberculosis complex]	Mycobacterium tuberculosis complex	62.8	62.8	45%	6e-14	50.00%	158	WP_003418034.1
hypothetical protein RVBD_3216 [Mycobacterium tuberculosis H37Rv]	Mycobacterium tuberculosis H37Rv	33.1	33.1	35%	0.003	40.38%	110	AFN51217.1

- Rim J:

Description	Scientific Name	Max Score	Total Score	Query Cover	E value	Per. Ident	Acc. Len	Accession
GNAT family N-acetyltransferase [Mycobacterium tuberculosis complex]	Mycobacterium tuberculosis complex	79.0	79.0	95%	4e-19	27.51%	217	WP_003898681.1
GNAT family N-acetyltransferase [Mycobacterium tuberculosis complex]	Mycobacterium tuberculosis complex	77.4	77.4	92%	1e-18	27.72%	203	WP_003405148.1

- Rim L:

Description	Scientific Name	Max Score	Total Score	Query Cover	E value	Per. Ident	Acc. Len	Accession
GNAT family N-acetyltransferase [Mycobacterium tuberculosis complex]	Mycobacterium tuberculosis complex	32.7	32.7	49%	0.011	25.84%	218	WP_003404111.1

B

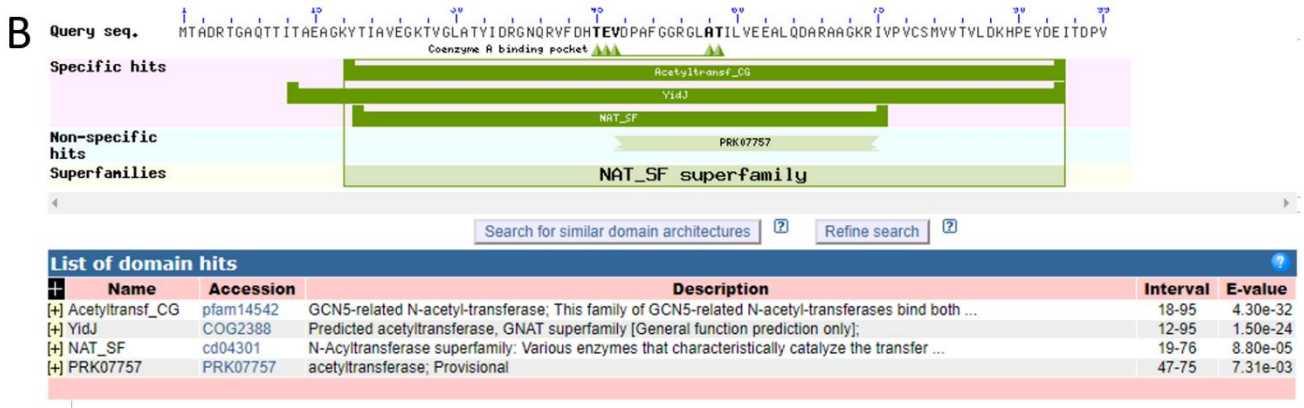

Name	Accession	Description	Interval	E-value
[+] Acetyltransf_CG	pfam14542	GCN5-related N-acetyl-transferase; This family of GCN5-related N-acetyl-transferases bind both ...	18-95	4.30e-32
[+] YidJ	COG2388	Predicted acetyltransferase, GNAT superfamily [General function prediction only];	12-95	1.50e-24
[+] NAT_SF	cd04301	N-Acyltransferase superfamily: Various enzymes that characteristically catalyze the transfer ...	19-76	8.80e-05
[+] PRK07757	PRK07757	acetyltransferase; Provisional	47-75	7.31e-03

C

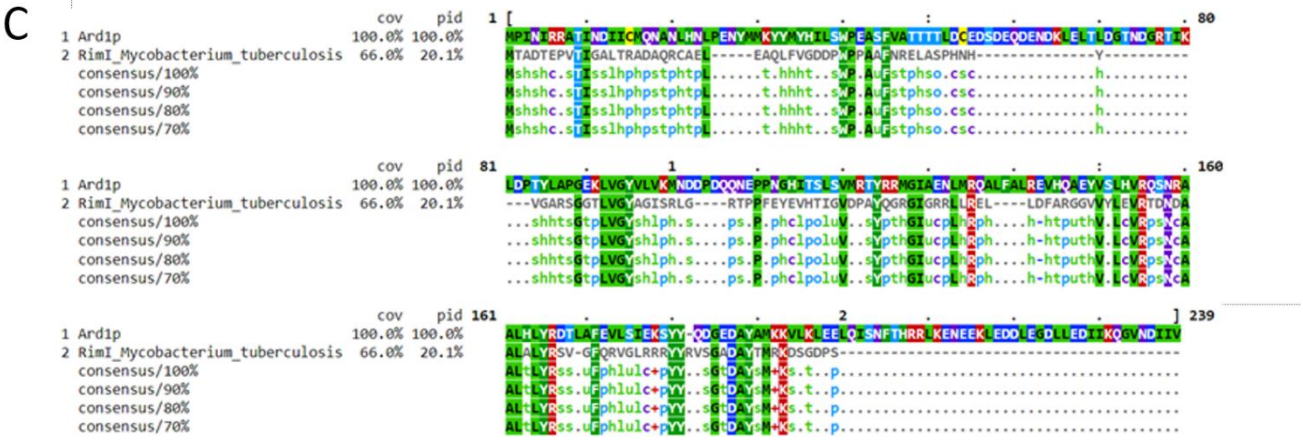

Figure 15. RimI Is Selected as Best Candidate for Acetylation of EsxA.

A) The RimI, RimJ and RimL proteins from *Pseudomonas aureginosa* were used to blast against H37Rv Mtb. The e-value for RimI and RimJ showed confidence in the hits received. B) The MMAR_0039 protein is analyzed using the domain search tool from NCBI. C) The RimI protein is the closest match to the Ard1p catalytic subunit.

3.3.1 Bioinformatic Analysis Reveals RimI as the Best Candidate for Acetylation of EsxA.

Given the importance of N-α acetylation in the overall virulence of Mm as found in this study and the influence it has on the membrane lytic activity of the EsxA:B heterodimer, identifying a possible enzyme responsibly for catalyzing the interaction might serve as a therapeutic target. In previous studies, RimI, RimJ, and RimL were found to be common bacterial N-α-acetyltransferases (128, 130). After a blast(p), it was revealed these 3 proteins had a homologue in Mtb (Fig. 15A). Furthermore, the previously implicated MMAR_0039 protein was analyzed using the domain search tool from NCBI (Fig. 15B), revealing it formed part of the NAT_SF superfamily which contain the Ard1p catalytic subunit. Next, the catalytic subunit was compared to the sequences of the Rim proteins and RimI contained the closest match (Fig. 15C). Upon research of these proteins RimI was isolated as a non-specific enzyme which may acetylate more proteins in Mtb than previously thought (129). For this reason, RimI was selected for further study.

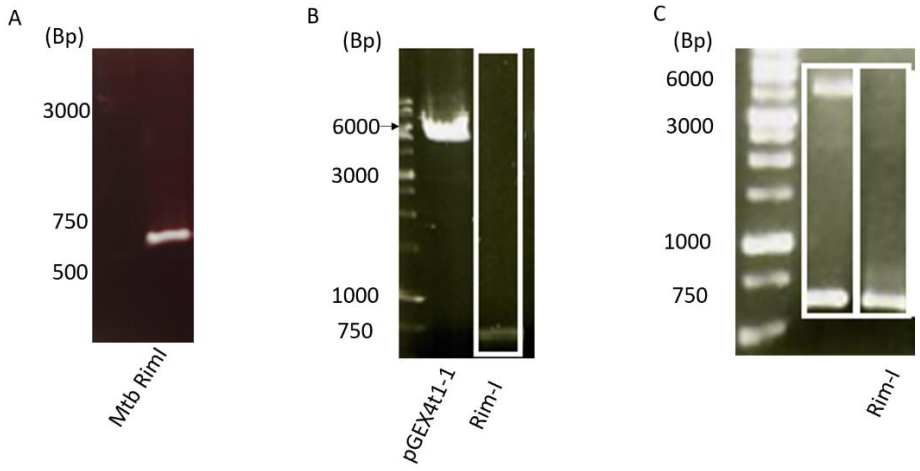

Figure 16. Generation of pET22b and pGEX-4T-1 Vector Containing RimI.

A) 1.0% agarose gel shows band at expected size after polymerase chain reaction using genomic Mtb DNA. B) pGEx-4T-1 plasmid and PCR products were digested. C) Following a transformation into *E. coli* d5ha cells, colonies were verified using double digestion, PCR product of RimI was used as a positive control.

3.3.2 Generation of pET22b and pGEX-4T-1 Vectors Containing RimI and Optimization of Expression.

The RimI protein was selected as the candidate for acetylation of EsxA, therefore the gene encoding for the RimI protein was amplified via PCR from genomic Mtb DNA (Fig. 16A). The resulting PCR product was then applied for the generation of the pET22b vector (result not shown) and pGEX-4T1 vectors (Fig. 16B, C). Both vectors have long been used and provide robust expression of proteins.

The vectors were then used in attempts to purify the gene through an array of conditions as outlined in tables 2. The conditions for expression in pET22b did not yield any successful expression of RimI. For this reason, we moved on to using the pGEX4t-1 vector, which expresses the target protein as a fusion protein with GST, typically resulting in solubilization of the target protein (131). As before, several different conditions were attempted as outlined in Table 2. Using lower temperatures post-induction resulted in the expression of the RimI protein as observed via SDS-PAGE (Fig. 17). To our surprise, soluble expression was not achieved using this vector, we therefore sought to move on to other vectors for expression.

Table 2. Expression Conditions Used with the pET22b and pGEX-4T-1 Vectors.

The different conditions used for expression of the RimI protein using either the pET22b or pGEX-4T-1 plasmids. Temperatures before induction (BI) and after induction (AI) were varied to improve changes of soluble expression. (* Denotes conditions with which expression of RimI was observed).

Plasmid	BI Temperature (°C)	OD600 Induced at	IPTG (mM)	Induction Time (Hours)	AI Temperature (°C)
pET22b	37	0.6	1	4	37
pET22b	37	0.6	1	8	16
pET22b	37	0.6	1	6	30
pET22b	37	0.6	0.1	8	16
pGEX-4T-1	37	0.6	1	8	37
pGEX-4T-1	37	0.6	0.1	8	37
pGEX-4T-1*	37	0.6	1	8	16
pGEX-4T-1*	30	0.6	1	8	16
pGEX-4T-1	37	1.5	1	8	16
pGEX-4T-1	37	2.5	1	8	16
pGEX-4T-1	37	0.6	1	6	30
pGEX-4T-1	37	0.6	1	4	37
pGEX-4T-1*	30, 30 startup	0.6	1	8	16

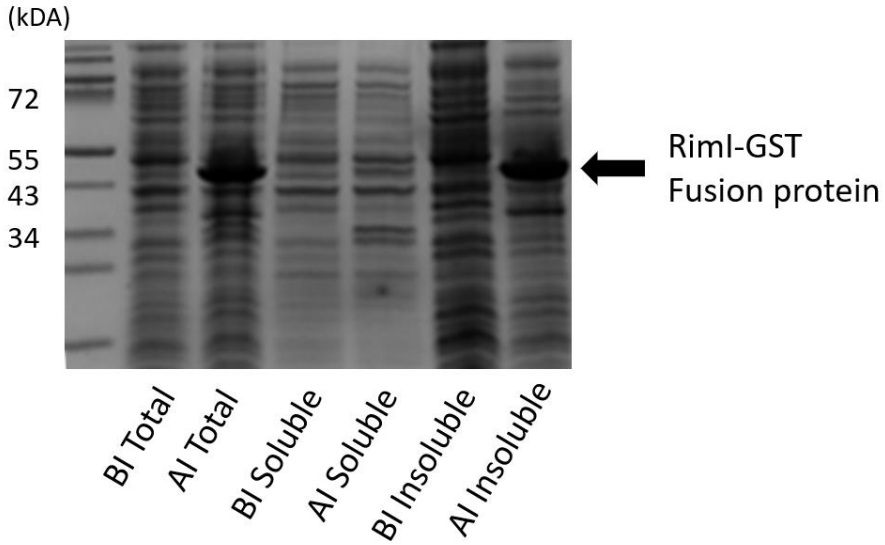

Figure 17. RimI Expression Using the pGEX-4T-1 Vector in Bl21 *E. coli* Cells.

The bacterial samples were assayed using B-PER to produce a total cell lysate, soluble proteins from supernatant and insoluble proteins from cell lysate. The samples were compared before induction (BI) and after induction (AI) using 1mM IPTG. RimI fusion proteins are labelled with an arrow theoretical protein size was expected at 45.5Kda and was observed below the 55kDA protein mark and above the 43kDa protein marker in a 15% tris-tricine gel. Soluble expression was not achieved using this vector.

3.3.3 Generation of a pET28b Plasmid Containing the RimI Protein and Expression in *E. Coli*.

Following the inability to obtain soluble expression of the RimI protein using the previous vectors, we decided to move on to the pET28b plasmid. Previous reports successfully used the pET28b plasmid for expression of RimI, and we therefore sought to replicate the conditions. Using the recently generated RimI gene, it was inserted into the NdeI and XhoI sites of the pET28b plasmid (Fig. 18).

Following the generation of the pET28b harboring the RimI gene, expression was then attempted under various conditions as outlined in table 3. After several attempts using different conditions, we were still not able to successfully express the RimI protein in *E. coli.*

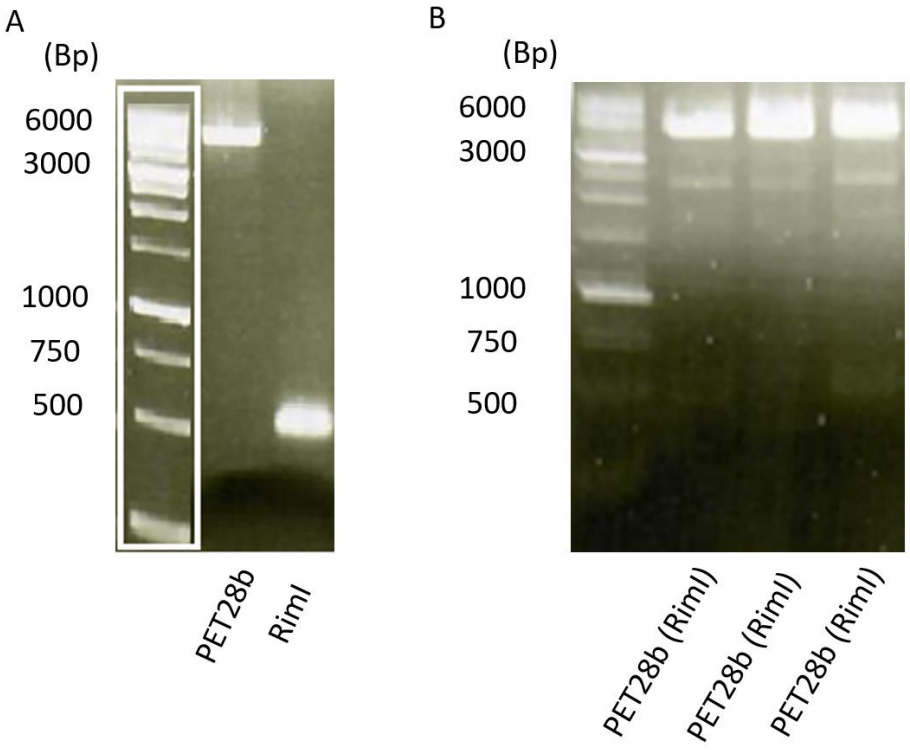

Figure 18. Generation of pET28b-TF Plasmid Containing RimI

A) pET28B plasmid and RimI PCR product were double digested. B) Following a transformation into d5ha cells, colonies were verified using a double digestion. Positive samples were then verified via DNA sequencing.

Table 3. Conditions Used for Expression of RimI in a pET28b Vector.

The various conditions used to express the RimI protein, none of these conditions yielded expression of the RimI protein. Temperatures before induction (BI) and after induction (AI) were varied to improve changes of soluble expression.

Plasmid	BI Temperature (°C)	OD600 Induced at	IPTG (mM)	Induction Time (Hours)	AI Temperature (°C)
pET28b	37	0.6	1	4	37
pET28b	37	0.6	1	6	30
pET28b	37	0.6	1	16	16
pET28b	37	1.4	1	4	37
pET28b	37	1.4	1	6	30
pET28b	37	1.4	1	16	16
pET28b	37	0.6	0.1	4	37
pET28b	37	0.6	0.1	6	30
pET28b	37	0.6	0.1	16	16
pET28b	37	1.4	0.1	4	37
pET28b	37	1.4	0.1	6	30
pET28b	37	1.4	0.1	16	16

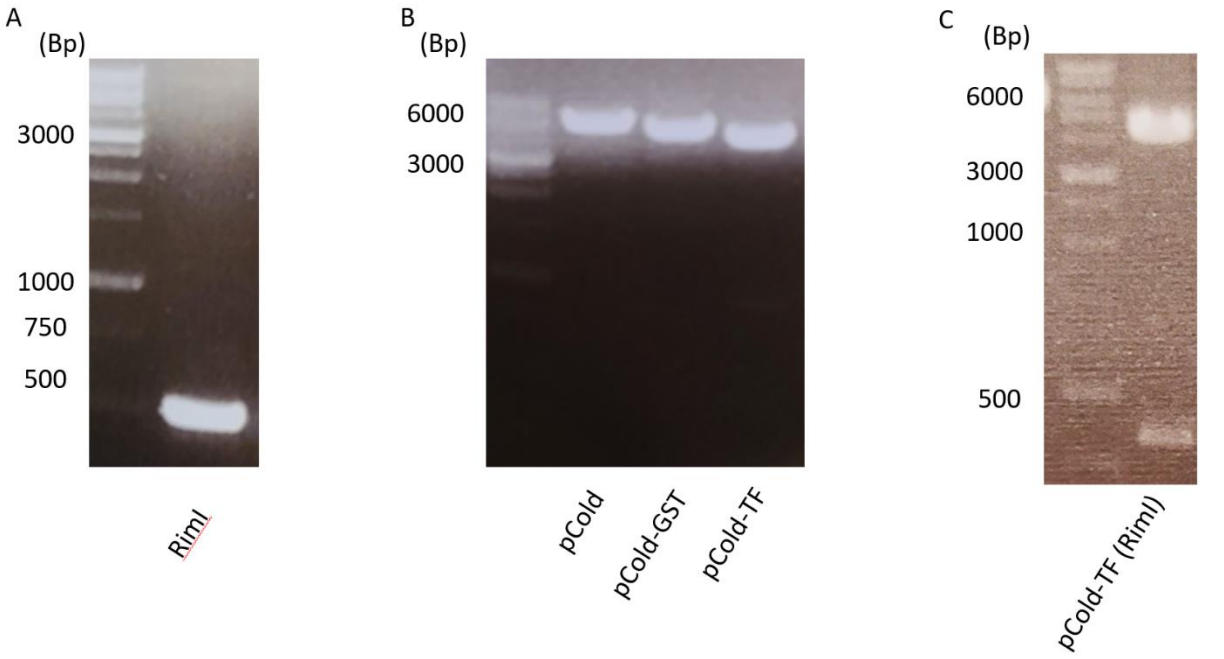

Figure 19. RimI Gene Was Inserted in the pCold-TF Vector.

A) RimI gene containing the NcoI and HindIII restriction sites was generated via PCR. B) The pCOLD, pCOLD-GST and pCOLD-TF vectors were double digested using NcoI and HindIII. C) RimI protein was inserted into the pCold-TF vector as verified via double digestion. Samples were confirmed via DNA sequencing.

3.3.4 RimI Was Purified Through Chromatography Using a Trigger Factor (TF) Fusion.

The purification of RimI was challenging with many different vectors being explored at a large number of conditions. We therefore turned to the pCOLD vector as another attempt to express the gene in *E coli.* We used the pCOLD, pCOLD-GST, and pCOLD-TF vectors and were able to insert the gene successfully into the pCOLD-TF vector(Fig. 19). The sequence was further confirmed via DNA sequencing.

RimI protein was then expressed using as previous, this time using only induction temperatures at 16°C. Furthermore, we obtained the Lemo21 (DE3) competent *E. coli* strain (NEB CAT#C2528J) which contains the Lemo System^{tm} for tunable expression of proteins. Prior to culturing, L-rhamnose was added to a final 0.5µM concentration, which slows down the expression in the Lemo21 competent cells. The cultures were grown at 37°C, 200 RPM, until OD_{600} 0.4-0.8. At this point they were cooled down with ice and induced with 1 mM IPTG. The cultures were allowed to continue to grow at 16°C, 150 RPM, for 24-48 hours; these conditions yielded soluble expression of RimI (Fig. 20A). The cells were harvested by centrifugation and sonicated. The soluble cell lysate was spun down at 15,000 RPM for 1 hour. The soluble fraction, supernatant was applied to 5mL HiTrap^{tm} TALON® crude columns and purified by metal affinity chromatography using an imidazole gradient as described in methods. SDS-PAGE revealed the purified RimI protein with TF fusion (Fig. 20B). Successful purification opened the opportunity to test whether the acetylation of EsxA was performed by the RimI enzyme.

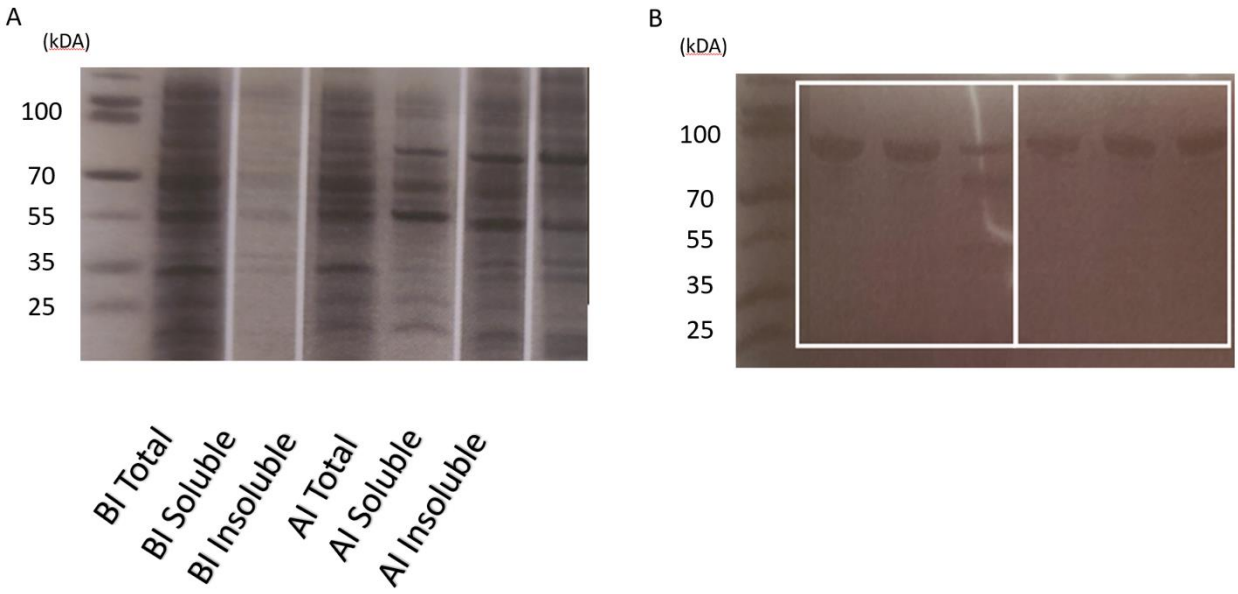

Figure 20. RimI Under the Control of a Tac and Cold Promoter Expressed in Lemo21 Cells.

A) RimI and TF fusion protein expression using pCOLD-TF in *E. coli* Lemo21 cells and 0.5µM rhamnose. Samples were tested for expression using B-PER, where total, soluble and insoluble fractions were obtained and compare before induction (BI) to after induction (AI). Theoretical protein size was expected and observed at approximately 79.5Kda in a 15% tris-tricine gel. B) Cells were lysed with sonication and purified using a TALON® crude column and fractionated using an AKTA prime plus, fractions containing a pure RimI protein as observed via SDS-PAGE.

3.3.5 The Purified RimI-TF Fusion Protein Was Not Able to Acetylate Proteins *In vitro.*

Following the purification of the RimI-TF fusion protein, the enzyme was used to test whether it was able to acetylate the EsxA gene. As a positive control for the study, the N-α-peptide of the NatC substrate, MLRYFRR, was used. This peptide was previously found to be acetylated with high affinity by RimI (129).

To test the extent of acetylation, a DTNB reagent based assayed was carried out after *in vitro* as previously described with a few modifications (129). Namely the concentration of peptide and EsxA protein was reduced to 1mM after initial attempts at 4mM. The concentration of RimI was also varied at either 8µM and 4µM for both EsxA and NatC substrate peptide. Negative control consisting of BSA protein as well as one lacking RimI was also prepared. Through this assay we discovered the Rim-I TF fusion protein was not able to acetylate either EsxA or the NATC

peptide (Fig. 21). Multiple attempts were carried out; however, none was successful, suggesting the RimI protein did not contain relaxed substrate specificity as previously thought. Our result was consistent with the findings of another group (132).

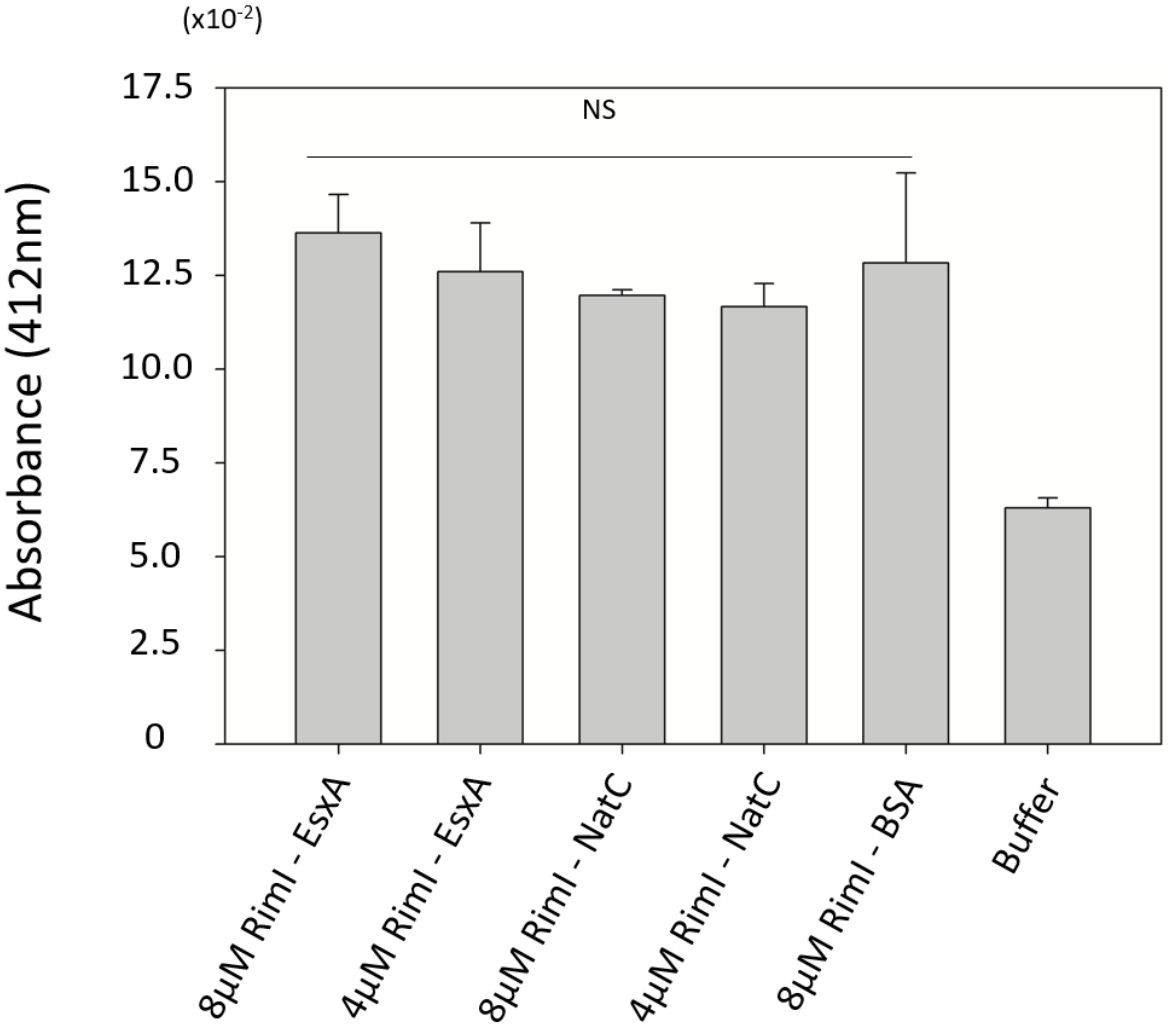

Figure 21. *In vitro* Acetylation of EsxA with RimI.

An acetylation reaction was carried out using RimI, the NatC substrate was used as a positive control while a negative control lacked RimI. There was no increase in the OD_{412} of any of the samples, revealing the acetylation reaction was not successful. This represents the average of 3 separate experiments, error bars show SD, $p < 0.05$.

3.4 Discussion

In this study, we focused on investigating the potential involvement of the RimI protein in the acetylation of EsxA, a crucial virulence factor in *Mycobacterium tuberculosis* (Mtb). To assess the acetylation activity of RimI towards EsxA, we employed the DTNB (5,5'-dithiobis(2-nitrobenzoic acid)) assay, a well-established method for detecting acetyltransferase activity (133). Contrary to our initial hypothesis, our results demonstrated that RimI did not acetylate EsxA.

This finding raises important questions regarding the presence of other acetyltransferases that may be involved in the regulation of EsxA acetylation. Furthermore, our study explored the substrate specificity of RimI towards other peptides, revealing no evidence of relaxed substrate specificity. This observation suggests that RimI may have a more specific and narrowly defined role in acetylating a limited range of protein substrates within the bacterial cell.

Our results are consistent with those from another study, which also found that the RimI protein did not acetylate EsxA or previously implicated peptides (132). Interestingly, the same study identified two other enzymes, MMAR_1067 and MMAR_1968 from *Mycobacterium marinum*, which were capable of acetylating EsxA (132). This finding highlights the possibility of alternative enzymes from Mtb which may be responsible for EsxA acetylation, and subsequently have a role in the pathogenesis of Mtb.

It is worth noting that protein acetylation has been successfully targeted for therapeutic purposes in various diseases. For instance, histone deacetylase inhibitors (HDACi) have been developed to target aberrant acetylation in cancer cells, leading to the approval of drugs such

as vorinostat, romidepsin, and belinostat for the treatment of certain types of cancer (134). Additionally, HDACi have shown promise in the treatment of neurodegenerative disorders such as Alzheimer's and Parkinson's diseases, where they modulate histone acetylation and other cellular processes to exert neuroprotective effects (135).

Although our results did not support the initial hypothesis regarding RimI's involvement in EsxA acetylation, our study rules out interactions with RimI. Moreover, it emphasizes the need for additional studies aimed at identifying the enzyme(s) in Mtb responsible for EsxA acetylation, as understanding this regulatory mechanism is critical for elucidating Mtb virulence and developing novel therapeutic strategies against tuberculosis. Given the successful targeting of acetylation in other disease contexts, this line of research may uncover new opportunities for drug development in the fight against Mtb infections.

Chapter 4: Specific Aim III: Express and Purify Prohibitin-1 Protein to Study its Interaction with EsxA.

4.1 Introduction

The EsxA protein is a strong virulence factor of Mtb which appears to play many roles in the virulence of Mtb (35, 47, 60, 77-80). While the role of EsxA as an effector protein for phagosomal escape of Mtb is well documented, less is known about what EsxA's function becomes once Mtb translocation occurs (47, 61). Previous studies have demonstrated the strong immune response EsxA can create due to its ability to interact with a plethora of host proteins (77-80).

Interestingly, some of the previous reports show EsxA interacting with host mitochondria pathways (80). Once such example is the role of EsxA in the mechanistic target of rapamycin (mTOR) (80). There are more studies which implicate EsxA interactions with host mitochondria (136). Through a pulldown assay of epithelial lung cells our group discovered the PHB1 protein pulls down with EsxA as well as the EsxA:B heterodimer and may be interacting partners (95).

Given that the prohibitin-1 and -2 proteins form a complex oligomer and have a set of roles in the mitochondria, they are often associated with many other host proteins (90, 91, 137-139). Additionally, PHB1 and PHB2 have also been the targets of pathogens (92-94). Our study went on to discover that knockdown of PHB1 enhances *Mycobacterium marinum* invasion and upregulates its intracellular survival (95). Together, these findings suggest PHB1 and PHB2 directly interact with EsxA.

Understanding the interaction between these two proteins could shed light on the mechanisms of the ESX-1 secretion system and its role in Mtb pathogenesis, as well as provide new insights

into the role of PHB1 and PHB2 in bacterial metabolism and virulence. By exploring the potential interaction between these two proteins in the context of their interactions with host mitochondrial proteins, we hope to uncover new insights into the complex interplay between Mtb and host cells during infection. In this aim purification methods for the PHB-1 protein are explored. Being able to purify the proteins will pave the way for novel studies.

4.2 Methods

4.2.1 Construction of Vectors

PHB1 and a PHB1 gene containing a deletion of the first 36 amino acids (PHB1Δ36) gene were isolated from a previously generated pCold-GST plasmid containing the PHB1 gene via PCR. PCR samples were purified using a PCR clean up kit (Thermo Cat#K310001). The genes were inserted into the NdeI and XhoI sites into pET22b, the BamH1 and EcoRI site in pGEX-4T-1, and the EcoRI and HindIII site in pMAL-c2X vectors. All clones were verified using DNA sequencing.

Table 4. Primers Used for Generation of Vectors Containing the PHB1 and PHB1Δ36 Proteins.

List of primers used in the study to clone PHB1 and PHB1Δ36 protein genes into the pET22b, pGEX-4t-1, and pMAL-c2X vectors.

Vector	F-Primer	R-Primer
pET22b PHB1	CCGGCATATGGCTGCCAAAGTGTTTGA	CCGGCTCGAGTCACTGGGGCAGCTGGA
pGEX-4t-1 PHB1	CGGGATCCATGGCTGCCAAAGTGTTTGA	CCCTCGAGTCACTGGGGCAGCTGGAG
pMAL-c2X PHB1	CCGGGAATTCATGGCTGCCAAAGTGTTTGA	CCGGAAGCTTTCACTGGGGCAGCTGGA
pET22b PHB1Δ36	CCGGCATATGGTCATCTTTGACCGATTCC	CCGGCTCGAGTCACTGGGGCAGCTGGA
pGEX-4t-1 PHB1Δ36	CCGGGGATCCATGGTCATCTTTGACCGATTCC	CCCTCGAGTCACTGGGGCAGCTGGAG
pMAL-c2X PHB1Δ36	CCGGGAATTCATGGTCATCTTTGACCGATTCC	CCGGAAGCTTTCACTGGGGCAGCTGGA

4.2.2 Expression of PhB1 in pET22b, pGEX-4T-1 and pMAL-c2X Plasmids.

To analyze the expression of the PHB1 protein, different plasmids such as pET22b, pGEX-4t-1, or pMAL-c2X were used to transform either *E. coli* BL21(DE3) or Lemo21 strains with PHB1 or PHB1Δ36. A single colony of the transformed bacteria was inoculated into 5 mL of LB broth supplemented with carbenicillin and incubated at 37°C with shaking at 220 RPM overnight. Subsequently, the overnight culture was used to inoculate 50 mL of LB broth supplemented with carbenicillin (100µg/ml) in a 250 mL flask and grown at 37°C with shaking at 220 RPM until the OD_{600} reached 0.6 to 0.8. To induce the expression of PHB1 proteins they were first cooled using ice, then IPTG was added to the culture at a final concentration of 1 mM, and the culture was allowed to continue to grow at 16°C while shaking at 150RPM. The bacteria were harvested by centrifugation at 5,000 x g for 10 minutes at 4°C. To lyse the cells, 300µl of bacterial protein extraction reagent (B-PER^{tm}) was used. A 50 µl sample was retained to observe the total lysate sample. The remaining lysate was centrifuged at 15,000RPM for 10 minutes at 4°C to pellet the insoluble fraction. The supernatant containing the soluble fraction was transferred to a clean microcentrifuge tube. Finally, all samples were subjected to SDS-PAGE analysis to observe for soluble expression. For more sensitive application, the PHB1 protein expressed in the pGEX-4T1-1 vector were observed via immunoblotting. The total and insoluble fractions were diluted 20-fold prior to loading into SDS-PAGE. They were then proved using α-PHB1 antibody.

4.2.3 Purification of PHB1 and PHB1Δ36 in pMAL-c2X Vector

The pMAL-c2X-PHB1 and PHB1Δ36 constructs were transformed into Lemo21 cells. A single colony was inoculated into 5 mL of LB broth containing 100 µg/mL carbenicillin and incubated overnight at 37°C with shaking at 200 RPM. The overnight culture was then used to inoculate 1L

LB broth containing 100 µg/mL carbenicillin, 1mM L-rhamnose, and grown at 37°C with shaking at 200 RPM until the OD_{600} reached 0.6. The cells were then cooled on ice and induced with IPTG at a concentration of 1 mM and incubated at 16°C with shaking at 150 RPM for 24 hours. The cells were harvested by centrifugation at 8,000 RPM for 10 minutes at 4°C. The cell pellet was resuspended in lysis buffer (20 mM Tris-HCl, 200 mM NaCl, 1 mM EDTA, pH 8.0) containing a protease inhibitor cocktail (Pierce™ Cat #32965) and sonicated on ice for 10 minutes pulsing on and off for 5 seconds and 9 seconds, respectively. The cell lysate was then centrifuged at 15,000 RPM for 45 minutes at 4°C to remove cell debris. Using a peristaltic pump, the clarified cell lysate was loaded onto a 15 mL amylose resin column pre-equilibrated with column buffer (20 mM Tris-HCl, 200 mM NaCl, 1 mM EDTA, pH 8.0). The samples were eluted using an AKTA FPLC pre-equilibrated with column buffer and elution buffer (10 mM maltose in column buffer), on a 100 mL gradient from 0% - 100% elution buffer. The eluted protein fractions were collected and analyzed by SDS-PAGE.

4.3 Results

4.3.1 Generation of pET22B Vectors Containing PHB1 and PHB1Δ36

The PHB1 protein consists of a large number of hydrophobic residues, for this reason we figured the purification of the protein would be difficult. To combat this, we sought to work with the full length PHB1 as well as a truncated PHB1 containing a deletion of the first 36 amino acids (PHB1Δ36). Due to their robust performance, the PHB-1 and PHB-1Δ36 proteins were inserted into the NdeI and XhoI sites of the pET22b vector, using the previously generated pCOLD-GST vectors containing PHB1 or PHB1Δ36 (Fig. 22).

4.3.2 Expression of PHB1 and PHB1Δ36 in the pET22B and pCold-GST Vectors

Following the generation of the pET22b and pCold-GST vectors, their expression was tested. In pET22b expression was observed in the insoluble fraction for the PHB1Δ36 gene (Fig. 23A). Expression was not observed for the full length PHB1 protein (Fig.23A). Expression was achieved by insertion of the plasmid into *E. coli* Bl21(De3) and culturing at 37°C until OD_{600} reached 0.6, at which point the proteins were induced with 1mM IPTG. The samples were then left to continue growing for 3 hours. The cells were then harvested by centrifugation.

We then moved onto expression of the PHB1 proteins in the pGEX-4t-1 plasmid and failed to achieve soluble expression as observable via SDS-PAGE. We therefore decided to immunoblot to see if any expression of the PHB1 protein was achievable. Total and insoluble fractions were diluted 20-fold prior to loading and after probing with αPHB1 antibody, soluble expression was observed for both proteins (Fig. 23B, C).

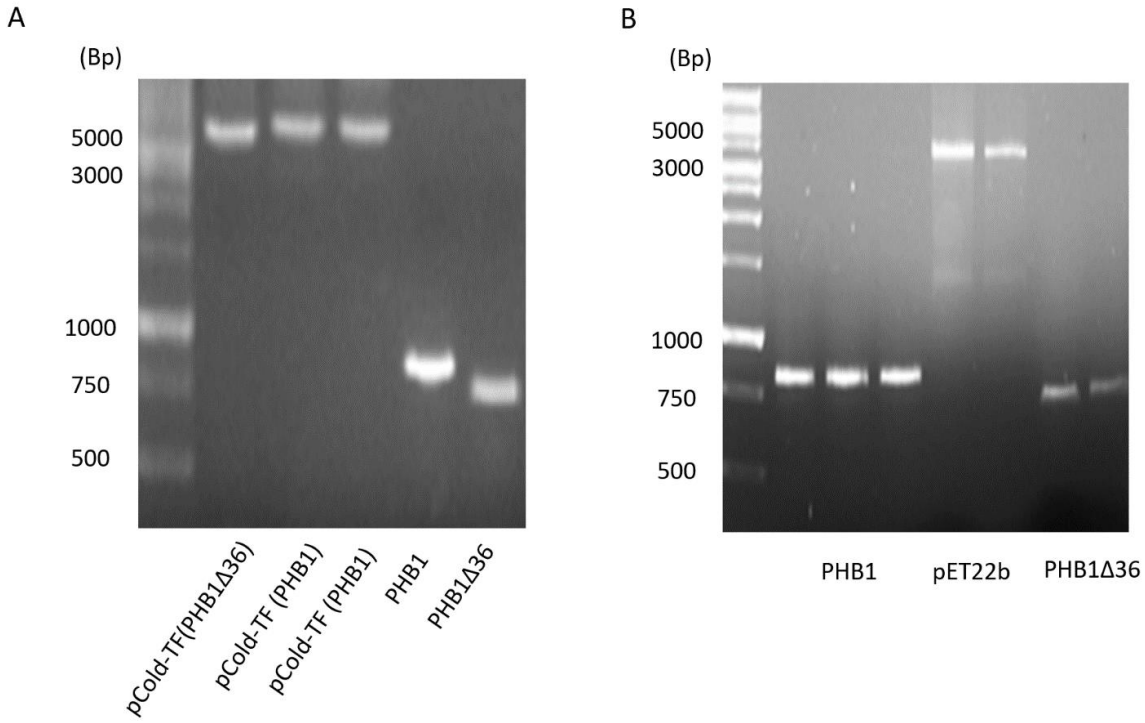

Figure 22. Generation of pET22-b and pCold-GST Vectors Containing the PHB1 Gene.

(A) The PHB1 and PHB1Δ36 genes were amplified via PCR from pCOLD-GST vector B) The PHB1 and PHB1Δ36 genes were double digested and used to generate the pET22b vector and confirmed via DNA sequencing.

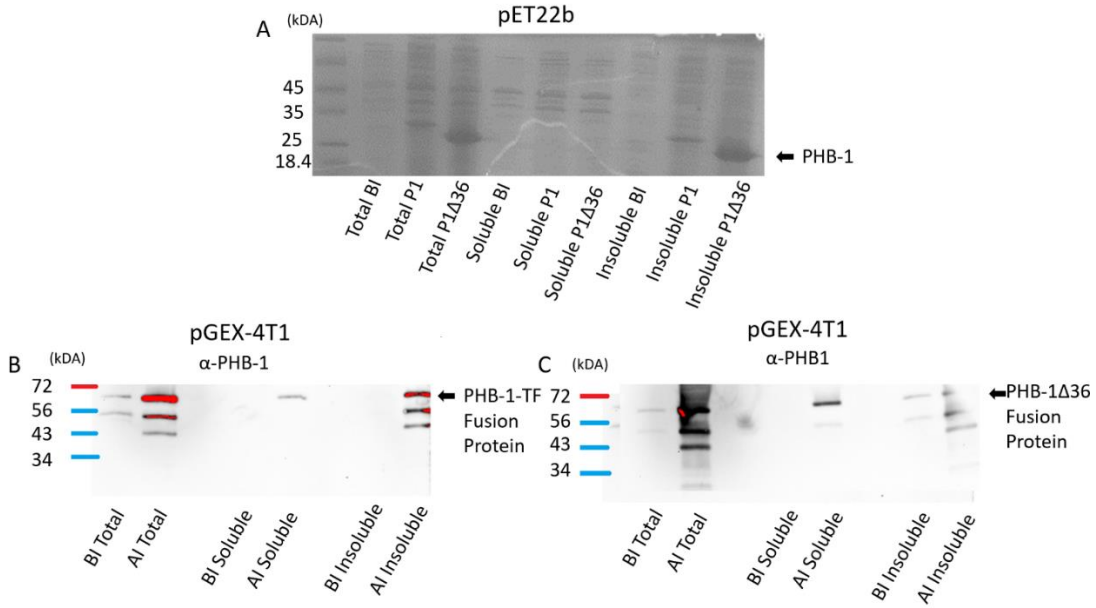

Figure 23. Expression of the PHB1 and PHB1Δ36 Genes in the pCold-GST Vector.

A) The PHB1Δ36 gene showed expression in the pET22b vector, albeit insoluble. The full length PHB1 gene did not show any expression. B) Samples were loaded into an SDS-PAGE and compared for expression before induction (BI) and after induction (AI). The SDS-PAGE was used for immunoblotting and soluble expression was appreciated in the pGEX-4t-1 vector with a slightly higher expression observed in the PHB1Δ36 protein.

4.3.3 Generation of pMAL-c2X Plasmid Containing PHB1 and PHB1Δ36 Gene and Purification of PHB1 Proteins.

Following evidence of the soluble expression of the PHB1 protein (Fig. 23), we sought to improve the conditions of soluble expression. To do this, we moved on to use the pMAL-c2X vector which creates a fusion of the target protein and maltose binding protein MBP. MBP is capable of solubilizing other proteins to greater degree (140). The genes encoding PHB1 and PHB1Δ36 were cloned into the EcoR1 and HindIII sites of the pMAL-c2X plasmid (Fig. 24).

To further increase our chances of successfully expressing soluble PHB1 proteins, we expressed the vectors in *E. coli* Lemo21 cells with 1mM L-rhamnose throughout growth of the culture. The cells were harvested after 16 hours post induction at 16°C. Initial analysis of the cell lysates using B-PER^{tm} by SDS-PAGE revealed the presence of an overexpressed protein in the soluble fraction with an approximate molecular weight of 65 kDa, corresponding to the expected size of the PHB1 protein fused with the maltose-binding protein (MBP) (Fig. 25). Soluble expression was achieved without the presence of L-rhamnose, although to a lesser extent.

To obtain the PHB1 protein we purified it using amylose resin. The cells were lysed using sonication at 70% amplitude, and the soluble fraction of the lysate was obtained after centrifugation. The lysate was subjected to amylose resin chromatography and eluted with 10mM maltose. To assess the purity of MBP-PHB1 protein, we performed an SDS-PAGE analysis which revealed the target protein and some additional bands (Fig. 26). These initial purifications reveal the possibility of purification of the PHB1 protein, which in the future can be used for subsequent biochemical studies to elucidate its interaction with EsxA from Mtb.

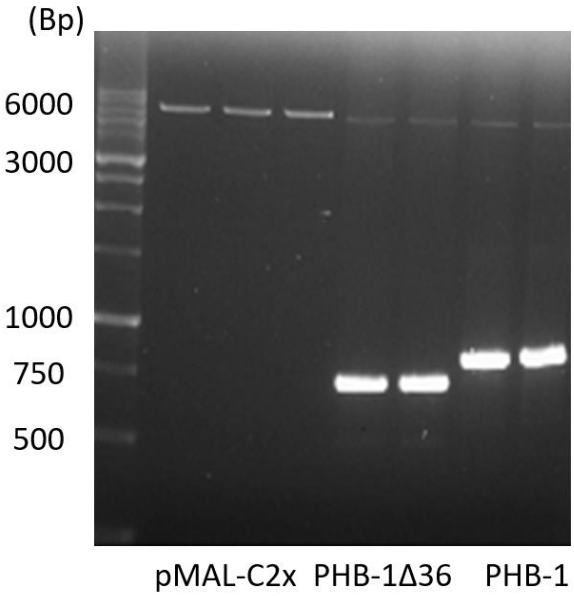

Figure 24. Generation of pMAL-c2X Vectors Containing the PHB-1 or PHB-1Δ36 Gene.

A) The pMAL-c2X vector was digested along with the PHB-1 gene, and the PHB-1 gene containing a deletion of the first 36 amino acids using EcoR1 and HindIII. The clones were verified via DNA sequencing.

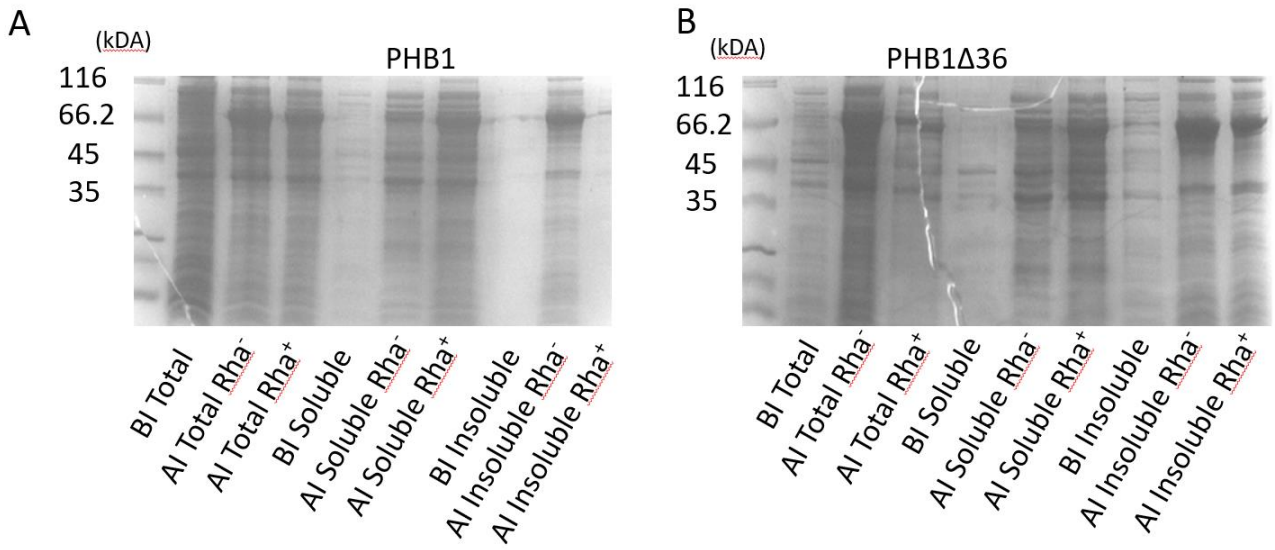

Figure 25. Expression of the PHB1 Gene Using the pMAL-c2X Vectors.

A) The pMAL-c2X vector was expressed using the Lemo21 cells with (Rha^+) or without L-rhamnose (Rha^-). B) The pMAL-c2X containing the PHB1Δ36 gene was expressed using the Lemo21 cells with or without L-rhamnose.

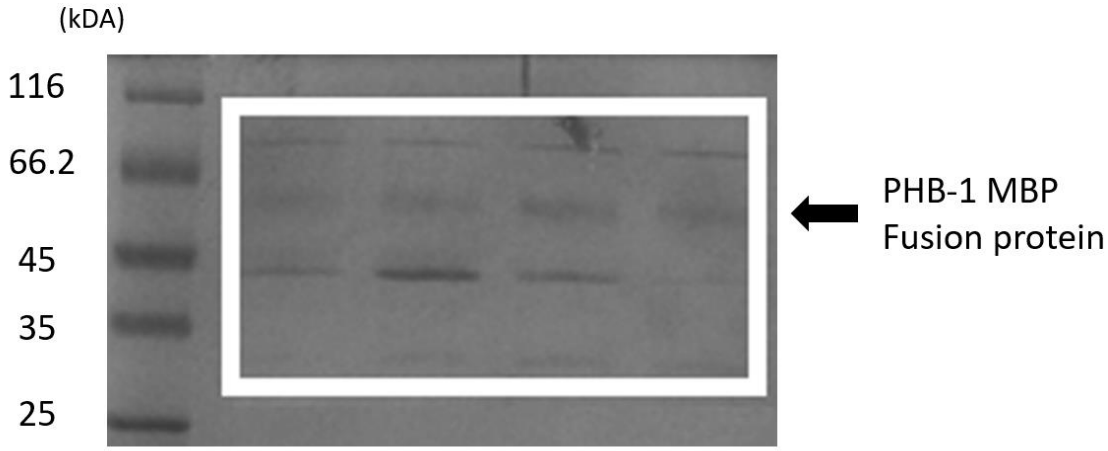

Figure 26. SDS-PAGE Analysis of the PHB1 Protein Using Amylose Resin.

The gel image displays the SDS-PAGE analysis of the purified PHB1 protein fractions obtained during the purification process. A band was observed below the 66.2 kDa marker consistent with the size of the PHB1 fused with MBP.

4.4 Discussion

In this study, we successfully purified PHB1 using amylose resin, which selectively binds to proteins fused to maltose binding protein (MBP) tags. Our strategy involved cloning the PHB1 gene into pMAL-c2X with an MBP tag, which allowed for purification of the PHB1-MBP fusion protein. SDS-PAGE analysis confirmed purity of the PHB1-MBP fusion protein, with an apparent molecular weight of ~70 kDa. Other bands were still present in the SDS-PAGE, but these may be the result of free-MBP. Furthermore, the PHB1 and PHB2 proteins are known for their ability to form complex oligomers, and the different bands might be indicative of different oligomerization states (84).

The purified protein of interest will be used to study its interactions with EsxA. Understanding of the interaction between these two proteins could shed light on the mechanisms of the ESX-1 secretion system and its role in bacterial pathogenesis. In previous studies, it was discovered

EsxA may interact with host mitochondrial proteins (80, 136). Furthermore, the pulldown of PHB1 and PHB2 with EsxA, as well as the enhanced virulence of *Mycobacterium marinum* following a PHB1 knockdown suggests these EsxA directly interacts with the prohibitin proteins (95).

In conclusion, the successful purification of both PHB1 and the protein of interest is an important step towards elucidating the interactions between EsxA and PHB1. Given the similarity PHB2 has with PHB1, it may be possible to translate the purification methods to PHB2. The purified proteins will lead to increased understanding of the complex interactions between EsxA and prohibitin proteins. Furthermore, it may also serve as a catalyst for the development of novel therapeutics against Mtb.

Chapter 5: Conclusions and Future Directions

In conclusion, our study has revealed important insights into the critical role of N-α-acetylation of EsxA in mycobacterial cytosolic translocation and virulence. Our findings also revealed that the acetylation status of EsxA results in differential binding to EsxB, which further emphasizes the critical role of acetylation in EsxA interactions with its molecular chaperone. Along the way of this study, we discovered a method to dissociate EsxA from EsxB *in vitro.* This finding opens the way for future research in Mtb. Furthermore, this study also leads to the conclusion that EsxA dissociation from EsxB is not only important, but essential for the cytolytic ability of EsxA. This study also provides compelling evidence for the role that N-α-acetylation plays in the pH dependent dissociation and its overall role in the virulence of Mtb.

Our results also provide strong evidence that EsxA acetylation is essential for efficient translocation of the protein into the host cell cytosol, and that this modification is crucial for mycobacterial pathogenesis. The discovery of the importance of EsxA acetylation suggests this modification could potentially serve as a novel therapeutic target for tuberculosis.

Moreover, our study has ruled out RimI as being responsible for the acetylation of EsxA, which suggests the presence of a unique acetyltransferase enzyme in Mtb responsible for this modification. Future studies aimed at identifying the specific enzyme responsible for EsxA acetylation could provide valuable insights into the mechanism underlying this modification and its impact on host-pathogen interactions.

Finally, this study lays the groundwork for studies on interactions between EsxA and PHB1 and PHB2 proteins. These future studies reveal potential new targets for developing novel therapeutics for mycobacterial infections and further elucidates the complex interactions EsxA

can form with host protesin. The identification of these interactions provides a better understanding of the molecular basis of mycobacterial pathogenesis and could pave the way for the development of new drugs that target these interactions.

Overall, our findings contribute to a better understanding of the molecular mechanisms underlying mycobacterial pathogenesis and virulence. Our results highlight the importance of acetylation in EsxA interactions with EsxB. Furthermore, it can be concluded that EsxA does not interact with the RimI protein. Future studies may further elucidate the role of EsxA acetylation and the enzyme which acetylates EsxA at its N-terminus. Lastly, our group has found strong evidence of EsxA interacting with PHB1 and PHB2. This study has found a lead for purification of the PHB1 in bacterial models. This model provides a more accessible option to produce the PHB1 protein, and due to its similarity, might also be translatable to PHB2. Successful purification of the prohibitin proteins will help identify the interactions between these proteins and EsxA. As a whole, this study has provided valuable insights in the interactions between EsxA and EsxB as a result of N-α acetylation, discards RimI as the enzyme responsible for acetylation, and lays the foundation for studying the host interactions with the PHB1 and PHB2 proteins.

References

1. World Health Organization. Global Tuberculosis Report 2021. [Internet]. [accessed March 7, 2023]. Available from: https://www.who.int/teams/global-tuberculosis-programme/global-report-2021.
2. World Health Organization. TB in Africa. [Internet]. [accessed March 7, 2023]. Available from: https://www.afro.who.int/health-topics/tuberculosis-tb
3. Mayo Clinic. Tuberculosis (TB). [Internet]. [accessed March 7, 2023]. Available from: https://www.mayoclinic.org/diseases-conditions/tuberculosis/symptoms-causes/syc-20351250.
4. Centers for Disease Control and Prevention. How TB Spreads. [Internet]. [accessed March 7, 2023]. Available from: https://www.cdc.gov/tb/topic/basics/howtbspreads.htm
5. Esmail, H., Riou, C., du Bruyn, E., Lai, R. P. J., Harley, Y. X., Meintjes, G., ... & Wilkinson, R. J. (2018). The immune response to Mycobacterium tuberculosis in HIV-1-coinfected persons. Annual review of immunology, 36, 603-638.
6. Pontillo A, Carvalho MS, Kamada AJ, Moura R, Schindler HC, Duarte AJ, Crovella S. Susceptibility to Mycobacterium tuberculosis infection in HIV-positive patients is associated with CARD8 genetic variant. JAIDS Journal of Acquired Immune Deficiency Syndromes. 2013 Jun 1;63(2):147-51.
7. Karim SS, Churchyard GJ, Karim QA, Lawn SD. HIV infection and tuberculosis in South Africa: an urgent need to escalate the public health response. the Lancet. 2009 Sep 12;374(9693):921-33.
8. Centers for Disease Control and Prevention. Mycobacterium tuberculosis (TB) Fact Sheet. [Internet]. [accessed March 7, 2023]. Available from: https://www.cdc.gov/tb/topic/basics/default.htm.
9. Centers for Disease Control and Prevention. Mycobacterium tuberculosis (TB) Fact Sheet. [Internet]. [accessed March 7, 2023]. Available from: https://www.cdc.gov/tb/topic/treatment/tbdisease.htm.
10. Centers for Disease Control and Prevention. Extensively drug-resistant tuberculosis (XDR TB). Available from: https://www.cdc.gov/tb/publications/factsheets/drtb/xdrtb.htm. Accessed 7 March 2023.
11. Rossi I, Bettini R, Buttini F. Resistant tuberculosis: the latest advancements of second-line antibiotic inhalation products. Current Pharmaceutical Design. 2021 Apr 1;27(12):1436-52.
12. Migliori GB, Sotgiu G, Gandhi NR, Falzon D, DeRiemer K, Centis R, Hollm-Delgado MG, Palmero D, Pérez-Guzmán C, Vargas MH, D'Ambrosio L. Drug resistance beyond extensively drug-resistant tuberculosis: individual patient data meta-analysis. European Respiratory Journal. 2013 Jul 1;42(1):169-79.
13. Udwadia ZF, Amale RA, Ajbani KK, Rodrigues C. Totally drug-resistant tuberculosis in India. Clinical Infectious Diseases. 2012 Feb 15;54(4):579-81.

14. Velayati AA, Masjedi MR, Farnia P, Tabarsi P, Ghanavi J, ZiaZarifi AH, Hoffner SE. Emergence of new forms of totally drug-resistant tuberculosis bacilli: super extensively drug-resistant tuberculosis or totally drug-resistant strains in Iran. Chest. 2009 Aug 1;136(2):420-5.
15. Ahmed MM, Velayati AA, Mohammed SH. Epidemiology of multidrug-resistant, extensively drug resistant, and totally drug resistant tuberculosis in Middle East countries. International journal of mycobacteriology. 2016 Sep 1;5(3):249-56.
16. Yadav S, Kapley A. Antibiotic resistance: Global health crisis and metagenomics. Biotechnology Reports. 2021 Mar 1;29:e00604.
17. World Health Organization. BCG Vaccine. [Internet]. [accessed March 7, 2023]. Available from: https://www.who.int/teams/health-product-policy-and-standards/standards-and-specifications/vaccines-quality/bcg
18. Parida SK, Axelsson-Robertson R, Rao MV, Singh N, Master I, Lutckii A, Keshavjee S, Andersson J, Zumla A, Maeurer M. Totally drug-resistant tuberculosis and adjunct therapies. Journal of internal medicine. 2015 Apr;277(4):388-405.
19. Colditz GA, Brewer TF, Berkey CS, Wilson ME, Burdick E, Fineberg HV, Mosteller F. Efficacy of BCG vaccine in the prevention of tuberculosis: meta-analysis of the published literature. Jama. 1994 Mar 2;271(9):698-702.
20. Milstien JB, Gibson JJ. Quality control of BCG vaccine by WHO: a review of factors that may influence vaccine effectiveness and safety. Bulletin of the World Health organization. 1990;68(1):93.
21. Martin C. The dream of a vaccine against tuberculosis; new vaccines improving or replacing BCG?. European Respiratory Journal. 2005 Jul 1;26(1):162-7.
22. Bahr GM, Stanford JL, Rook GA, Rees RJ, Abdelnoor AM, Frayha GJ. Two potential improvements to BCG and their effect on skin test reactivity in the Lebanon. Tubercle. 1986 Sep 1;67(3):205-18.
23. Glynn JR, Fielding K, Mzembe T, Sichali L, Banda L, McLean E, Kanjala C, Crampin AC, Ponnighaus JM, Warndorff DK, Fine PE. BCG re-vaccination in Malawi: 30-year follow-up of a large, randomised, double-blind, placebo-controlled trial. The Lancet Global health. 2021 Oct 1;9(10):e1451-9.
24. Rodrigues LC, Pereira SM, Cunha SS, Genser B, Ichihara MY, de Brito SC, Hijjar MA, Cruz AA, Sant'Anna C, Bierrenbach AL, Barreto ML. Effect of BCG revaccination on incidence of tuberculosis in school-aged children in Brazil: the BCG-REVAC cluster-randomised trial. The Lancet. 2005 Oct 8;366(9493):1290-5.
25. Dantas OM, de A Ximenes RA, de FPM de Albuquerque M, da Silva NL, Montarroyos UR, de Souza WV, Pereira TC, Campelo AR, Rodrigues LC. A case-control study of protection against tuberculosis by BCG revaccination in Recife, Brazil. The international journal of tuberculosis and lung disease. 2006 May 1;10(5):536-41.
26. World Health Organization. Global Tuberculosis Programme. [Internet]. [accessed March 7, 2023]. Available from: https://www.who.int/teams/global-tuberculosis-programme/research-innovation/vaccines

27. Tait DR, Hatherill M, Van Der Meeren O, Ginsberg AM, Van Brakel E, Salaun B, Scriba TJ, Akite EJ, Ayles HM, Bollaerts A, Demoitié MA. Final analysis of a trial of M72/AS01E vaccine to prevent tuberculosis. New England Journal of Medicine. 2019 Dec 19;381(25):2429-39.
28. Cotton MF, Madhi SA, Luabeya AK, Tameris M, Hesseling AC, Shenje J, Schoeman E, Hatherill M, Desai S, Kapse D, Brückner S. Safety and immunogenicity of VPM1002 versus BCG in South African newborn babies: A randomised, phase 2 non-inferiority double-blind controlled trial. The Lancet Infectious Diseases. 2022 Oct 1;22(10):1472-83.
29. Behr MA, Wilson MA, Gill WP, Salamon H, Schoolnik GK, Rane S, Small PM. Comparative genomics of BCG vaccines by whole-genome DNA microarray. Science. 1999 May 28;284(5419):1520-3.
30. Brosch R, Philipp WJ, Stavropoulos E, Colston MJ, Cole ST, Gordon SV. Genomic analysis reveals variation between Mycobacterium tuberculosis H37Rv and the attenuated M. tuberculosis H37Ra strain. Infection and immunity. 1999 Nov 1;67(11):5768-74.
31. Gordon SV, Brosch R, Billault A, Garnier T, Eiglmeier K, Cole ST. Identification of variable regions in the genomes of tubercle bacilli using bacterial artificial chromosome arrays. Molecular microbiology. 1999 May;32(3):643-55.
32. Chai Q, Wang L, Liu CH, Ge B. New insights into the evasion of host innate immunity by Mycobacterium tuberculosis. Cellular & Molecular Immunology. 2020 Sep;17(9):901-13.
33. Bespiatykh D, Bespyatykh J, Mokrousov I, Shitikov E. A comprehensive map of mycobacterium tuberculosis complex regions of difference. Msphere. 2021 Aug 31;6(4):e00535-21.
34. Chitale P, Lemenze AD, Fogarty EC, Shah A, Grady C, Odom-Mabey AR, Johnson WE, Yang JH, Eren AM, Brosch R, Kumar P. A comprehensive update to the M ycobacterium tuberculosis H37Rv reference genome. Nature communications. 2022 Nov 18;13(1):7068.
35. Fortune SM, Jaeger A, Sarracino DA, Chase MR, Sassetti CM, Sherman DR, Bloom BR, Rubin EJ. Mutually dependent secretion of proteins required for mycobacterial virulence. Proceedings of the National Academy of Sciences. 2005 Jul 26;102(30):10676-81.
36. Ganguly N, Siddiqui I, Sharma P. Role of M. tuberculosis RD-1 region encoded secretory proteins in protective response and virulence. Tuberculosis. 2008 Nov 1;88(6):510-7.
37. Lewis KN, Liao R, Guinn KM, Hickey MJ, Smith S, Behr MA, Sherman DR. Deletion of RD1 from Mycobacterium tuberculosis mimics bacille Calmette-Guerin attenuation. The Journal of infectious diseases. 2003 Jan 1;187(1):117-23.
38. Pym AS, Brodin P, Majlessi L, Brosch R, Demangel C, Williams A, Griffiths KE, Marchal G, Leclerc C, Cole ST. Recombinant BCG exporting ESAT-6 confers enhanced protection against tuberculosis. Nature medicine. 2003 May 1;9(5):533-9.
39. Mostowy S, Cousins D, Behr MA. Genomic interrogation of the dassie bacillus reveals it as a unique RD1 mutant within the Mycobacterium tuberculosis complex. Journal of bacteriology. 2004 Jan 1;186(1):104-9.

40. Abdallah AM, Gey van Pittius NC, DiGiuseppe Champion PA, Cox J, Luirink J, Vandenbroucke-Grauls CM, Appelmelk BJ, Bitter W. Type VII secretion—mycobacteria show the way. Nature reviews microbiology. 2007 Nov;5(11):883-91.
41. Houben EN, Korotkov KV, Bitter W. Take five—Type VII secretion systems of Mycobacteria. Biochimica et Biophysica Acta (BBA)-Molecular Cell Research. 2014 Aug 1;1843(8):1707-16.
42. Simeone R, Bottai D, Brosch R. ESX/type VII secretion systems and their role in host–pathogen interaction. Current opinion in microbiology. 2009 Feb 1;12(1):4-10.
43. Gröschel MI, Sayes F, Simeone R, Majlessi L, Brosch R. ESX secretion systems: mycobacterial evolution to counter host immunity. Nature Reviews Microbiology. 2016 Nov;14(11):677-91.
44. Reyes SV. Characterization of EsxA: EsxB Heterodimer Membrane Interaction with a Novel POPC/POPG Liposome Model (Doctoral dissertation, The University of Texas at El Paso).
45. De Leon J, Jiang G, Ma Y, Rubin E, Fortune S, Sun J. Mycobacterium tuberculosis ESAT-6 exhibits a unique membrane-interacting activity that is not found in its ortholog from non-pathogenic Mycobacterium smegmatis. Journal of Biological Chemistry. 2012 Dec 28;287(53):44184-91.
46. De Jonge MI, Pehau-Arnaudet G, Fretz MM, Romain F, Bottai D, Brodin P, Honoré N, Marchal G, Jiskoot W, England P, Cole ST. ESAT-6 from Mycobacterium tuberculosis dissociates from its putative chaperone CFP-10 under acidic conditions and exhibits membrane-lysing activity. Journal of bacteriology. 2007 Aug 15;189(16):6028-34
47. Zhang Q, Wang D, Jiang G, Liu W, Deng Q, Li X, Qian W, Ouellet H, Sun J. EsxA membrane-permeabilizing activity plays a key role in mycobacterial cytosolic translocation and virulence: effects of single-residue mutations at glutamine 5. Scientific reports. 2016 Sep 7;6(1):1-5.
48. Singh P, Benjak A, Schuenemann VJ, Herbig A, Avanzi C, Busso P, Nieselt K, Krause J, Vera-Cabrera L, Cole ST. Insight into the evolution and origin of leprosy bacilli from the genome sequence of Mycobacterium lepromatosis. Proceedings of the National Academy of Sciences. 2015 Apr 7;112(14):4459-64.
49. Serafini A, Boldrin F, Palu G, Manganelli R. Characterization of a Mycobacterium tuberculosis ESX-3 conditional mutant: essentiality and rescue by iron and zinc. Journal of bacteriology. 2009 Oct 15;191(20):6340-4.
50. Siegrist MS, Unnikrishnan M, McConnell MJ, Borowsky M, Cheng TY, Siddiqi N, Fortune SM, Moody DB, Rubin EJ. Mycobacterial Esx-3 is required for mycobactin-mediated iron acquisition. Proceedings of the National Academy of Sciences. 2009 Nov 3;106(44):18792-7.
51. Tufariello JM, Chapman JR, Kerantzas CA, Wong KW, Vilchèze C, Jones CM, Cole LE, Tinaztepe E, Thompson V, Fenyö D, Niederweis M. Separable roles for Mycobacterium tuberculosis ESX-3 effectors in iron acquisition and virulence. Proceedings of the National Academy of Sciences. 2016 Jan 19;113(3):E348-57.

52. Ates LS, van der Woude AD, Bestebroer J, van Stempvoort G, Musters RJ, Garcia-Vallejo JJ, Picavet DI, Weerd RV, Maletta M, Kuijl CP, van der Wel NN. The ESX-5 system of pathogenic mycobacteria is involved in capsule integrity and virulence through its substrate PPE10. PLoS Pathogens. 2016 Jun 9;12(6):e1005696.
53. Ates LS, Ummels R, Commandeur S, van der Weerd R, Sparrius M, Weerdenburg E, Alber M, Kalscheuer R, Piersma SR, Abdallah AM, Abd El Ghany M. Essential role of the ESX-5 secretion system in outer membrane permeability of pathogenic mycobacteria. PLoS genetics. 2015 May 4;11(5):e1005190.
54. Wang Q, Boshoff HI, Harrison JR, Ray PC, Green SR, Wyatt PG, Barry III CE. PE/PPE proteins mediate nutrient transport across the outer membrane of Mycobacterium tuberculosis. Science. 2020 Mar 6;367(6482):1147-51.
55. Phan TH, van Leeuwen LM, Kuijl C, Ummels R, van Stempvoort G, Rubio-Canalejas A, Piersma SR, Jiménez CR, van der Sar AM, Houben EN, Bitter W. EspH is a hypervirulence factor for Mycobacterium marinum and essential for the secretion of the ESX-1 substrates EspE and EspF. PLoS pathogens. 2018 Aug 13;14(8):e1007247.
56. Solomonson M, Setiaputra D, Makepeace KA, Lameignere E, Petrotchenko EV, Conrady DG, Bergeron JR, Vuckovic M, DiMaio F, Borchers CH, Yip CK. Structure of EspB from the ESX-1 type VII secretion system and insights into its export mechanism. Structure. 2015 Mar 3;23(3):571-83.
57. Ates LS, Brosch R. D iscovery of the type VII ESX-1 secretion needle?. Molecular Microbiology. 2017 Jan;103(1):7-12.
58. Renshaw PS, Panagiotidou P, Whelan A, Gordon SV, Hewinson RG, Williamson RA, Carr MD. Conclusive evidence that the major t-cell antigens of themycobacterium tuberculosis complex esat-6 and cfp-10 form a tight, 1: 1 complex and characterization of the structural properties of esat-6, cfp-10, and the esat-6· cfp-10 complex: Implications for pathogenesis and virulence. Journal of Biological Chemistry. 2002 Jun 14;277(24):21598-603.
59. Ma Y, Keil V, Sun J. Characterization of Mycobacterium tuberculosis EsxA membrane insertion: roles of N-and C-terminal flexible arms and central helix-turn-helix motif. Journal of Biological Chemistry. 2015 Mar 13;290(11):7314-22.
60. Bao Y, Wang L, Sun J. A small protein but with diverse roles: a review of EsxA in mycobacterium–host interaction. Cells. 2021 Jun 30;10(7):1645.
61. Simeone R, Sayes F, Song O, Gröschel MI, Brodin P, Brosch R, Majlessi L. Cytosolic access of Mycobacterium tuberculosis: critical impact of phagosomal acidification control and demonstration of occurrence in vivo. PLoS pathogens. 2015 Feb 6;11(2):e1004650.
62. Refai A, Haoues M, Othman H, Barbouche MR, Moua P, Bondon A, Mouret L, Srairi-Abid N, Essafi M. Two distinct conformational states of Mycobacterium tuberculosis virulent factor early secreted antigenic target 6 kD a are behind the discrepancy around its biological functions. The FEBS journal. 2015 Nov;282(21):4114-29.
63. Conrad WH, Osman MM, Shanahan JK, Chu F, Takaki KK, Cameron J, Hopkinson-Woolley D, Brosch R, Ramakrishnan L. Mycobacterial ESX-1 secretion system mediates host cell

lysis through bacterium contact-dependent gross membrane disruptions. Proceedings of the National Academy of Sciences. 2017 Feb 7;114(6):1371-6.
64. Okkels LM, Müller EC, Schmid M, Rosenkrands I, Kaufmann SH, Andersen P, Jungblut PR. CFP10 discriminates between nonacetylated and acetylated ESAT-6 of Mycobacterium tuberculosis by differential interaction. Proteomics. 2004 Oct;4(10):2954-60.
65. Starheim KK, Gevaert K, Arnesen T. Protein N-terminal acetyltransferases: when the start matters. Trends in biochemical sciences. 2012 Apr 1;37(4):152-61.
66. Ree R, Varland S, Arnesen T. Spotlight on protein N-terminal acetylation. Experimental & molecular medicine. 2018 Jul;50(7):1-3.
67. Arnesen T, Van Damme P, Polevoda B, Helsens K, Evjenth R, Colaert N, Varhaug JE, Vandekerckhove J, Lillehaug JR, Sherman F, Gevaert K. Proteomics analyses reveal the evolutionary conservation and divergence of N-terminal acetyltransferases from yeast and humans. Proceedings of the National Academy of Sciences. 2009 May 19;106(20):8157-62.
68. Geng H, Liu Q, Xue C, David LL, Beer TM, Thomas GV, Dai MS, Qian DZ. HIF1α protein stability is increased by acetylation at lysine 709. Journal of Biological Chemistry. 2012 Oct 12;287(42):35496-505.
69. Daitoku H, Sakamaki JI, Fukamizu A. Regulation of FoxO transcription factors by acetylation and protein–protein interactions. Biochimica et Biophysica Acta (BBA)-Molecular Cell Research. 2011 Nov 1;1813(11):1954-60.
70. Ishfaq M, Maeta K, Maeda S, Natsume T, Ito A, Yoshida M. Acetylation regulates subcellular localization of eukaryotic translation initiation factor 5A (eIF5A). FEBS letters. 2012 Sep 21;586(19):3236-41.
71. Wilson BJ, Tremblay AM, Deblois G, Sylvain-Drolet G, Giguere V. An acetylation switch modulates the transcriptional activity of estrogen-related receptor α. Molecular endocrinology. 2010 Jul 1;24(7):1349-58.
72. Jones JD, O'Connor CD. Protein acetylation in prokaryotes. Proteomics. 2011 Aug;11(15):3012-22.
73. Christensen DG, Baumgartner JT, Xie X, Jew KM, Basisty N, Schilling B, Kuhn ML, Wolfe AJ. Mechanisms, detection, and relevance of protein acetylation in prokaryotes. MBio. 2019 Apr 30;10(2):e02708-18.
74. Lopes da Rosa J, Boyartchuk VL, Zhu LJ, Kaufman PD. Histone acetyltransferase Rtt109 is required for Candida albicans pathogenesis. Proceedings of the National Academy of Sciences. 2010 Jan 26;107(4):1594-9.
75. Pathak SK, Basu S, Basu KK, Banerjee A, Pathak S, Bhattacharyya A, Kaisho T, Kundu M, Basu J. Direct extracellular interaction between the early secreted antigen ESAT-6 of Mycobacterium tuberculosis and TLR2 inhibits TLR signaling in macrophages. Nature immunology. 2007 Jun;8(6):610-8.
76. Schumann G, Schleier S, Rosenkrands I, Nehmann N, Hälbich S, Zipfel P, Jonge M, Cole S, Munder T, Möllmann U. Mycobacterium tuberculosis secreted protein ESAT-6 interacts with the human protein syntenin-1. Open Life Sciences. 2006 Jun 1;1(2):183-202.

77. Khan HS, Nair VR, Ruhl CR, Alvarez-Arguedas S, Galvan Rendiz JL, Franco LH, Huang L, Shaul PW, Kim J, Xie Y, Mitchell RB. Identification of scavenger receptor B1 as the airway microfold cell receptor for Mycobacterium tuberculosis. Elife. 2020 Mar 5;9:e52551.
78. Sreejit G, Ahmed A, Parveen N, Jha V, Valluri VL, Ghosh S, Mukhopadhyay S. The ESAT-6 protein of Mycobacterium tuberculosis interacts with beta-2-microglobulin (β2M) affecting antigen presentation function of macrophage. PLoS pathogens. 2014 Oct 30;10(10):e1004446.
79. Chatterjee S, Dwivedi VP, Singh Y, Siddiqui I, Sharma P, Van Kaer L, Chattopadhyay D, Das G. Early secreted antigen ESAT-6 of Mycobacterium tuberculosis promotes protective T helper 17 cell responses in a toll-like receptor-2-dependent manner. PLoS pathogens. 2011 Nov 10;7(11):e1002378.
80. Fine-Coulson K, Giguère S, Quinn FD, Reaves BJ. Infection of A549 human type II epithelial cells with Mycobacterium tuberculosis induces changes in mitochondrial morphology, distribution and mass that are dependent on the early secreted antigen, ESAT-6. Microbes and infection. 2015 Oct 1;17(10):689-97.
81. Songane M, Kleinnijenhuis J, Netea MG, van Crevel R. The role of autophagy in host defence against Mycobacterium tuberculosis infection. Tuberculosis. 2012 Sep 1;92(5):388-96.
82. Back JW, Sanz MA, De Jong L, De Koning LJ, Nijtmans LG, De Koster CG, Grivell LA, Van Der Spek H, Muijsers AO. A structure for the yeast prohibitin complex: Structure prediction and evidence from chemical crosslinking and mass spectrometry. Protein Science. 2002 Oct;11(10):2471-8.
83. Artal-Sanz M, Tavernarakis N. Prohibitin and mitochondrial biology. Trends in Endocrinology & Metabolism. 2009 Oct 1;20(8):394-401.
84. Tatsuta T, Model K, Langer T. Formation of membrane-bound ring complexes by prohibitins in mitochondria. Molecular biology of the cell. 2005 Jan;16(1):248-59.
85. Fusaro G, Dasgupta P, Rastogi S, Joshi B, Chellappan S. Prohibitin induces the transcriptional activity of p53 and is exported from the nucleus upon apoptotic signaling. Journal of Biological Chemistry. 2003 Nov 28;278(48):47853-61.
86. Sato T, Sakamoto T, Takita KI, Saito H, Okui K, Nakamura Y. The human prohibitin (PHB) gene family and its somatic mutations in human tumors. Genomics. 1993 Sep 1;17(3):762-4.
87. Mishra S, Ande SR, Nyomba BG. The role of prohibitin in cell signaling. The FEBS journal. 2010 Oct;277(19):3937-46.
88. Nuell MJ, Stewart DA, Walker L, Friedman V, Wood CM, Owens GA, Smith JR, Schneider EL, Dell'Orco R, Lumpkin CK. Prohibitin, an evolutionarily conserved intracellular protein that blocks DNA synthesis in normal fibroblasts and HeLa cells. Molecular and cellular biology. 1991 Mar;11(3):1372-81.
89. Zhou Z, Ai H, Li K, Yao X, Zhu W, Liu L, Yu C, Song Z, Bao Y, Huang Y, Wu Y. Prohibitin 2 localizes in nucleolus to regulate ribosomal RNA transcription and facilitate cell proliferation in RD cells. Scientific reports. 2018 Jan 24;8(1):1479.

90. Merkwirth C, Langer T. Prohibitin function within mitochondria: essential roles for cell proliferation and cristae morphogenesis. Biochimica et Biophysica Acta (BBA)-Molecular Cell Research. 2009 Jan 1;1793(1):27-32.
91. Nijtmans LG, de Jong L, Sanz MA, Coates PJ, Berden JA, Back JW, Muijsers AO, van der Spek H, Grivell LA. Prohibitins act as a membrane-bound chaperone for the stabilization of mitochondrial proteins. The EMBO journal. 2000 Jun 1;19(11):2444-51.
92. Sharma A, Qadri A. Vi polysaccharide of Salmonella typhi targets the prohibitin family of molecules in intestinal epithelial cells and suppresses early inflammatory responses. Proceedings of the National Academy of Sciences. 2004 Dec 14;101(50):17492-7.
93. Cornillez-Ty CT, Liao L, Yates III JR, Kuhn P, Buchmeier MJ. Severe acute respiratory syndrome coronavirus nonstructural protein 2 interacts with a host protein complex involved in mitochondrial biogenesis and intracellular signaling. Journal of virology. 2009 Oct 1;83(19):10314-8.
94. Wintachai P, Wikan N, Kuadkitkan A, Jaimipuk T, Ubol S, Pulmanausahakul R, Auewarakul P, Kasinrerk W, Weng WY, Panyasrivanit M, Paemanee A. Identification of prohibitin as a Chikungunya virus receptor protein. Journal of medical virology. 2012 Nov;84(11):1757-70.
95. Bao, Y, Sun, J. Prohibitin-1 is involved in mycobacterial invasion and survival in human lung epithelial cells. In preparation
96. Aguilera J, Karki CB, Li L, Reyes SV, Estevao I, Grajeda BI, Zhang Q, Arico CD, Ouellet H, Sun J. Nα-Acetylation of the virulence factor EsxA is required for mycobacterial cytosolic translocation and virulence. Journal of Biological Chemistry. 2020 Apr 24;295(17):5785-94.
97. Mba Medie F, Champion MM, Williams EA, Champion PA. Homeostasis of N-α-terminal acetylation of EsxA correlates with virulence in Mycobacterium marinum. Infection and immunity. 2014 Nov;82(11):4572-86.
98. Aguilera JA. Investigation Into the Role of N-terminal Acetylation of ESAT-6 in Pathogenesis of Mycobacterium tuberculosis. The University of Texas at El Paso; 2017.
99. Scroggins BT, Robzyk K, Wang D, Marcu MG, Tsutsumi S, Beebe K, Cotter RJ, Felts S, Toft D, Karnitz L, Rosen N. An acetylation site in the middle domain of Hsp90 regulates chaperone function. Molecular cell. 2007 Jan 12;25(1):151-9.
100. Mukherjee S, Hao YH, Orth K. A newly discovered post-translational modification–the acetylation of serine and threonine residues. Trends in biochemical sciences. 2007 May 1;32(5):210-6.
101. Jacquez P, Lei N, Weigt D, Xiao C, Sun J. Expression and purification of the functional ectodomain of human anthrax toxin receptor 2 in Escherichia coli Origami B cells with assistance of bacterial Trigger Factor. Protein expression and purification. 2014 Mar 1;95:149-55.
102. Sun J, Vernier G, Wigelsworth DJ, Collier RJ. Insertion of anthrax protective antigen into liposomal membranes: effects of a receptor. Journal of Biological Chemistry. 2007 Jan 12;282(2):1059-65.

103. Takaki K, Davis JM, Winglee K, Ramakrishnan L. Evaluation of the pathogenesis and treatment of Mycobacterium marinum infection in zebrafish. Nature protocols. 2013 Jun;8(6):1114-24.
104. Simeone R, Bobard A, Lippmann J, Bitter W, Majlessi L, Brosch R, Enninga J. Phagosomal rupture by Mycobacterium tuberculosis results in toxicity and host cell death. PLoS pathogens. 2012 Feb 2;8(2):e1002507.
105. Acosta Y, Zhang Q, Rahaman A, Ouellet H, Xiao C, Sun J, Li C. Imaging cytosolic translocation of Mycobacteria with two-photon fluorescence resonance energy transfer microscopy. Biomedical optics express. 2014 Nov 1;5(11):3990-4001.
106. Aguilera J, Sun J. Measuring Cytosolic Translocation of Mycobacterium marinum in RAW264. 7 Macrophages with a CCF4-AM FRET Assay. Bio-protocol. 2021 Apr 20;11(8):e3991-.
107. Renshaw PS, Lightbody KL, Veverka V, Muskett FW, Kelly G, Frenkiel TA, Gordon SV, Hewinson RG, Burke B, Norman J, Williamson RA. Structure and function of the complex formed by the tuberculosis virulence factors CFP-10 and ESAT-6. The EMBO journal. 2005 Jul 20;24(14):2491-8.
108. Wang L, Zhang M, Alexov E. DelPhiPKa web server: predicting p K a of proteins, RNAs and DNAs. Bioinformatics. 2016 Feb 15;32(4):614-5.
109. Humphrey W, Dalke A, Schulten K. VMD: visual molecular dynamics. Journal of molecular graphics. 1996 Feb 1;14(1):33-8.
110. Jorgensen WL, Chandrasekhar J, Madura JD, Impey RW, Klein ML. Comparison of simple potential functions for simulating liquid water. The Journal of chemical physics. 1983 Jul 15;79(2):926-35.
111. Phillips JC, Braun R, Wang W, Gumbart J, Tajkhorshid E, Villa E, Chipot C, Skeel RD, Kale L, Schulten K. Scalable molecular dynamics with NAMD. Journal of computational chemistry. 2005 Dec;26(16):1781-802.
112. Vanommeslaeghe K, Hatcher E, Acharya C, Kundu S, Zhong S, Shim J, Darian E, Guvench O, Lopes P, Vorobyov I, Mackerell Jr AD. CHARMM general force field: A force field for drug-like molecules compatible with the CHARMM all-atom additive biological force fields. Journal of computational chemistry. 2010 Mar;31(4):671-90.
113. Vazquez Reyes S, Ray S, Aguilera J, Sun J. Development of an in vitro membrane model to study the function of EsxAB Heterodimer and establish the role of EsxB in membrane permeabilizing activity of mycobacterium tuberculosis. Pathogens. 2020 Dec 2;9(12):1015.
114. Aguilera J, Vazquez-Reyes S, Sun J. A Fluorescence Dequenching-based Liposome Leakage Assay to Measure Membrane Permeabilization by Pore-forming Proteins. Bio-protocol. 2021 May 20;11(10):e4025-.
115. Zlokarnik G, Negulescu PA, Knapp TE, Mere L, Burres N, Feng L, Whitney M, Roemer K, Tsien RY. Quantitation of transcription and clonal selection of single living cells with β-lactamase as reporter. Science. 1998 Jan 2;279(5347):84-8.

116. Cavrois M, De Noronha C, Greene WC. A sensitive and specific enzyme-based assay detecting HIV-1 virion fusion in primary T lymphocytes. Nature biotechnology. 2002 Nov 1;20(11):1151-4.
117. Aguilera J, Sun J. Measuring Cytosolic Translocation of Mycobacterium marinum in RAW264. 7 Macrophages with a CCF4-AM FRET Assay. Bio-protocol. 2021 Apr 20;11(8):e3991-.
118. van der Wel N, Hava D, Houben D, Fluitsma D, van Zon M, Pierson J, Brenner M, Peters PJ. M. tuberculosis and M. leprae translocate from the phagolysosome to the cytosol in myeloid cells. Cell. 2007 Jun 29;129(7):1287-98.
119. Houben D, Demangel C, Van Ingen J, Perez J, Baldeón L, Abdallah AM, Caleechurn L, Bottai D, Van Zon M, De Punder K, Van Der Laan T. ESX-1-mediated translocation to the cytosol controls virulence of mycobacteria. Cellular microbiology. 2012 Aug;14(8):1287-98.
120. Hsu T, Hingley-Wilson SM, Chen B, Chen M, Dai AZ, Morin PM, Marks CB, Padiyar J, Goulding C, Gingery M, Eisenberg D. The primary mechanism of attenuation of bacillus Calmette–Guerin is a loss of secreted lytic function required for invasion of lung interstitial tissue. Proceedings of the National Academy of Sciences. 2003 Oct 14;100(21):12420-5.
121. Ree R, Varland S, Arnesen T. Spotlight on protein N-terminal acetylation. Experimental & molecular medicine. 2018 Jul;50(7):1-3.
122. Drazic A, Myklebust LM, Ree R, Arnesen T. The world of protein acetylation. Biochimica et Biophysica Acta (BBA)-Proteins and Proteomics. 2016 Oct 1;1864(10):1372-401.3.
123. Liu F, Yang M, Wang X, Yang S, Gu J, Zhou J, Zhang XE, Deng J, Ge F. Acetylome analysis reveals diverse functions of lysine acetylation in Mycobacterium tuberculosis. Molecular & cellular proteomics. 2014 Dec 1;13(12):3352-66.
124. Bi J, Wang Y, Yu H, Qian X, Wang H, Liu J, Zhang X. Modulation of central carbon metabolism by acetylation of isocitrate lyase in Mycobacterium tuberculosis. Scientific reports. 2017 Mar 21;7(1):1-1.
125. Lee W, VanderVen BC, Walker S, Russell DG. Novel protein acetyltransferase, Rv2170, modulates carbon and energy metabolism in Mycobacterium tuberculosis. Scientific Reports. 2017 Mar 6;7(1):72.
126. Manzo F, Tambaro FP, Mai A, Altucci L. Histone acetyltransferase inhibitors and preclinical studies. Expert opinion on therapeutic patents. 2009 Jun 1;19(6):761-74.
127. Sievers F, Wilm A, Dineen D, Gibson TJ, Karplus K, Li W, Lopez R, McWilliam H, Remmert M, Söding J, Thompson JD. Fast, scalable generation of high-quality protein multiple sequence alignments using Clustal Omega. Molecular systems biology. 2011;7(1):539.
128. Yoshikawa A, Isono S, Sheback A, Isono K. Cloning and nucleotide sequencing of the genes rimI and rimJ which encode enzymes acetylating ribosomal proteins S18 and S5 of Escherichia coli K12. Molecular and General Genetics MGG. 1987 Oct;209:481-8

129. Pathak D, Bhat AH, Sapehia V, Rai J, Rao A. Biochemical evidence for relaxed substrate specificity of Nα-acetyltransferase (Rv3420c/rimI) of Mycobacterium tuberculosis. Scientific reports. 2016 Jun 29;6(1):1-2.
130. Tanka S, Matsushita Y, Yoshikawa A, Isono K. Cloning and molecular characterization of the gene rimL wich encodes an enzyme acetylating ribosomal protein L12 of Escherichia coki K12. Molecular and General Genetics MGG. 1989 Jun;217:289-93.
131. Frangioni JV, Neel BG. Solubilization and purification of enzymatically active glutathione S-transferase (pGEX) fusion proteins. Analytical biochemistry. 1993 Apr 1;210(1):179-87.
132. Ferrell MJ. Investigations of the Virulence Mechanisms of Mycobacterium marinum. University of Notre Dame; 2020.
133. Foyn H, Thompson PR, Arnesen T. DTNB-based quantification of in vitro enzymatic N-terminal acetyltransferase activity. Protein Terminal Profiling: Methods and Protocols. 2017:9-15.
134. Marks PA, Xu WS. Histone deacetylase inhibitors: Potential in cancer therapy. Journal of cellular biochemistry. 2009 Jul 1;107(4):600-8.
135. Fischer A, Sananbenesi F, Wang X, Dobbin M, Tsai LH. Recovery of learning and memory is associated with chromatin remodelling. Nature. 2007 May 10;447(7141):178-82.
136. Pagán AJ, Lee LJ, Edwards-Hicks J, Moens CB, Tobin DM, Busch-Nentwich EM, Pearce EL, Ramakrishnan L. mTOR-regulated mitochondrial metabolism limits mycobacterium-induced cytotoxicity. Cell. 2022 Sep 29;185(20):3720-38.
137. Strub GM, Paillard M, Liang J, Gomez L, Allegood JC, Hait NC, Maceyka M, Price MM, Chen Q, Simpson DC, Kordula T. Sphingosine-1-phosphate produced by sphingosine kinase 2 in mitochondria interacts with prohibitin 2 to regulate complex IV assembly and respiration. The FASEB Journal. 2011 Feb;25(2):600.
138. Salameh A, Daquinag AC, Staquicini DI, An Z, Hajjar KA, Pasqualini R, Arap W, Kolonin MG. Prohibitin/annexin 2 interaction regulates fatty acid transport in adipose tissue. JCI insight. 2016 Jul 7;1(10).
139. Wang S, Nath N, Adlam M, Chellappan S. Prohibitin, a potential tumor suppressor, interacts with RB and regulates E2F function. Oncogene. 1999 Jun;18(23):3501-10.
140. Sun P, Tropea JE, Waugh DS. Enhancing the solubility of recombinant proteins in Escherichia coli by using hexahistidine-tagged maltose-binding protein as a fusion partner. Heterologous Gene Expression in E. coli: Methods and Protocols. 2011:259-74.

Vita

Javier Aguilera began his career through advanced placement and dual enrollment at the El Paso Community College in his high school years. After obtaining his high school diploma he continued to the University of Texas at El Paso in Fall 2011. Upon taking general microbiology in the Summer of 2013, Javier joined Dr. Sun's laboratory through the Campus office of Undergraduate Research Initiatives (COURI).

Upon joining the laboratory in the Fall of 2013, Javier began to develop his project which he presented in several conferences to include the Annual Biomedical Research Conference for Minoritized Scientists (ABRCMS), American Society for Biochemistry and Molecular Biology (ASBMB) annual meeting, American Society of Microbiology (ASM), and multiple appearances at the COURI symposia. He then enrolled in the FAST track program and continued to earn his bachelor's degree of science in December 2014. He continued to work on a master's degree under the supervision of Dr. Sun, where he presented at the border biomedical research center symposium and the 5th Tuberculosis Research Symposium.

Javier then continued to work on his Ph.D. under the supervision of Dr. Sun, where he obtained support through the Research Initiative for Scientific Enhancement (RISE). He took part in many projects and obtained a first authorship publication in 2020. Throughout the 2020 pandemic, he collaborated in many projects which eventually led to the publication of two more first author publications in 2021. He also obtained 3 publications as a second author as a result of this work. Throughout his time at UTEP he mentored over 20 undergraduate students. Javier may be reached via email at: Javier.Aguilera25@outlook.com

This Dissertation was typed by Javier Aguilera.